Searches for Dark Matter produced in association with a Higgs boson and invisible decays of the observed Higgs boson using the ATLAS detector

XXVIII International Workshop on Deep-Inelastic Scattering and Related Subjects

14. 04. 2021

Alexander Leopold, on behalf of the ATLAS collaboration

ATLAS EXPERIMENT

DIS 2021

COPPE UFRJ

Evidence for Dark Matter

Strong evidence for dark matter from astrophysical and cosmological observations*)

Hints that non-luminous matter is needed*) to explain the observation is found on several scales

- galaxies ↠ rotation curves
- galaxy cluster collisions ↠ weak lensing
- cosmological scale ↠ CMB, large structure formation

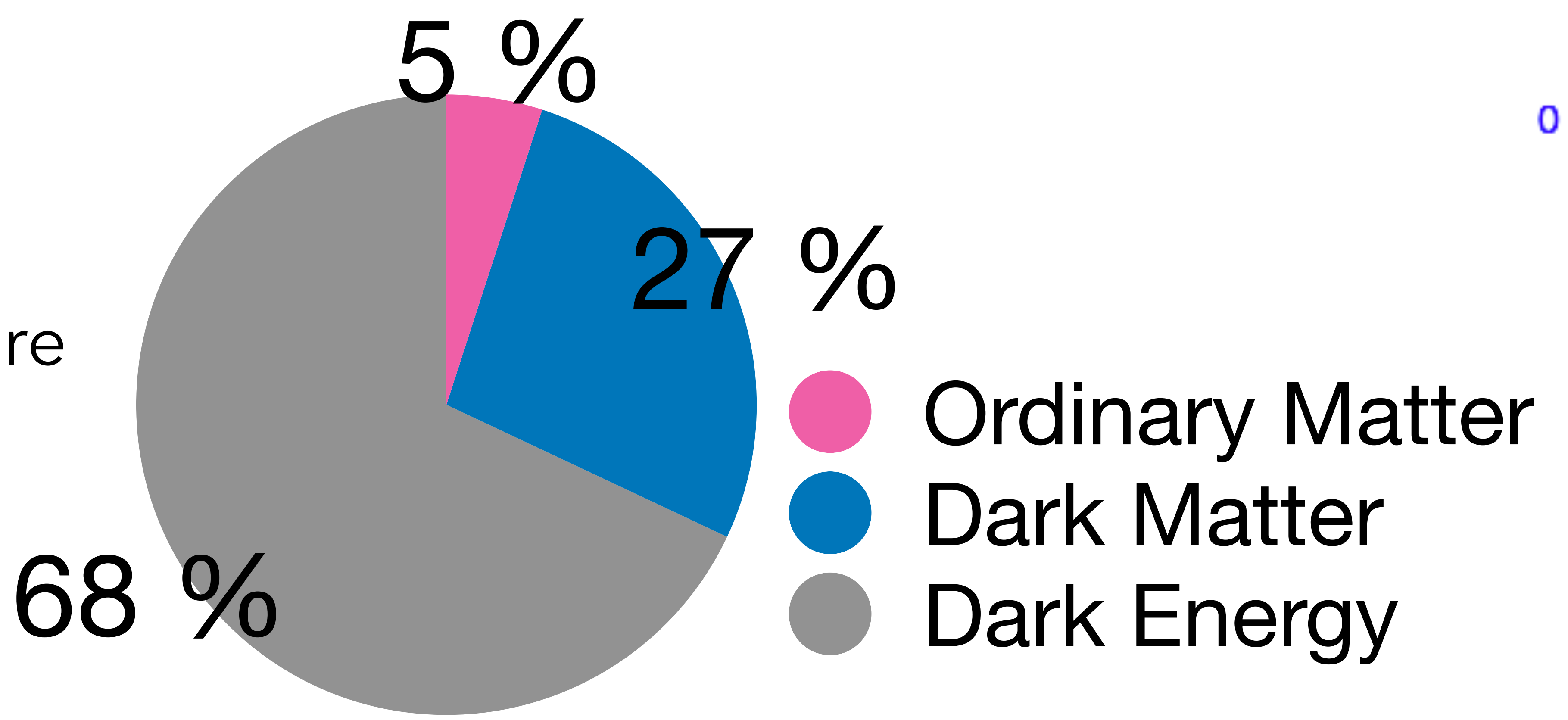

[Mon.Not.Roy.Astron.Soc. 311 (2000) 441-447]

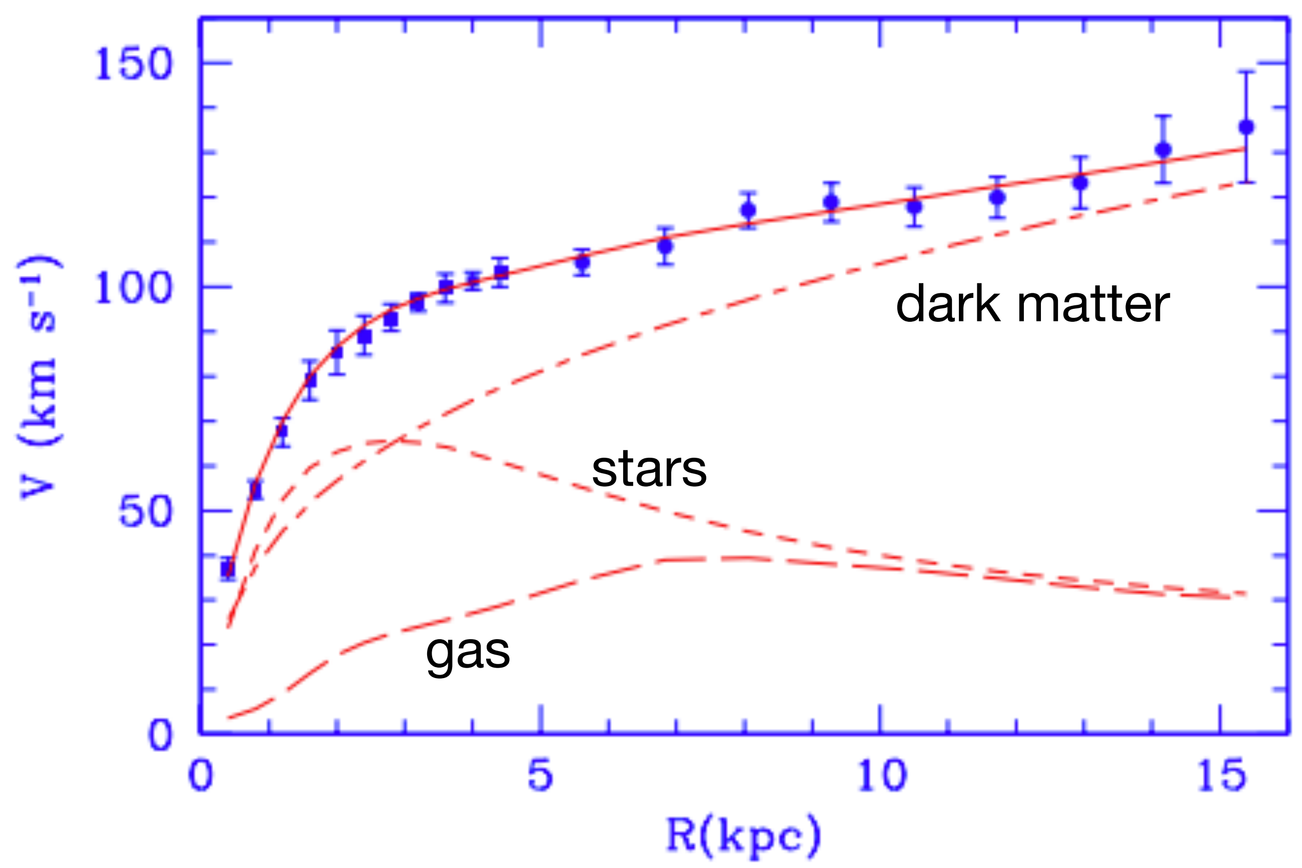

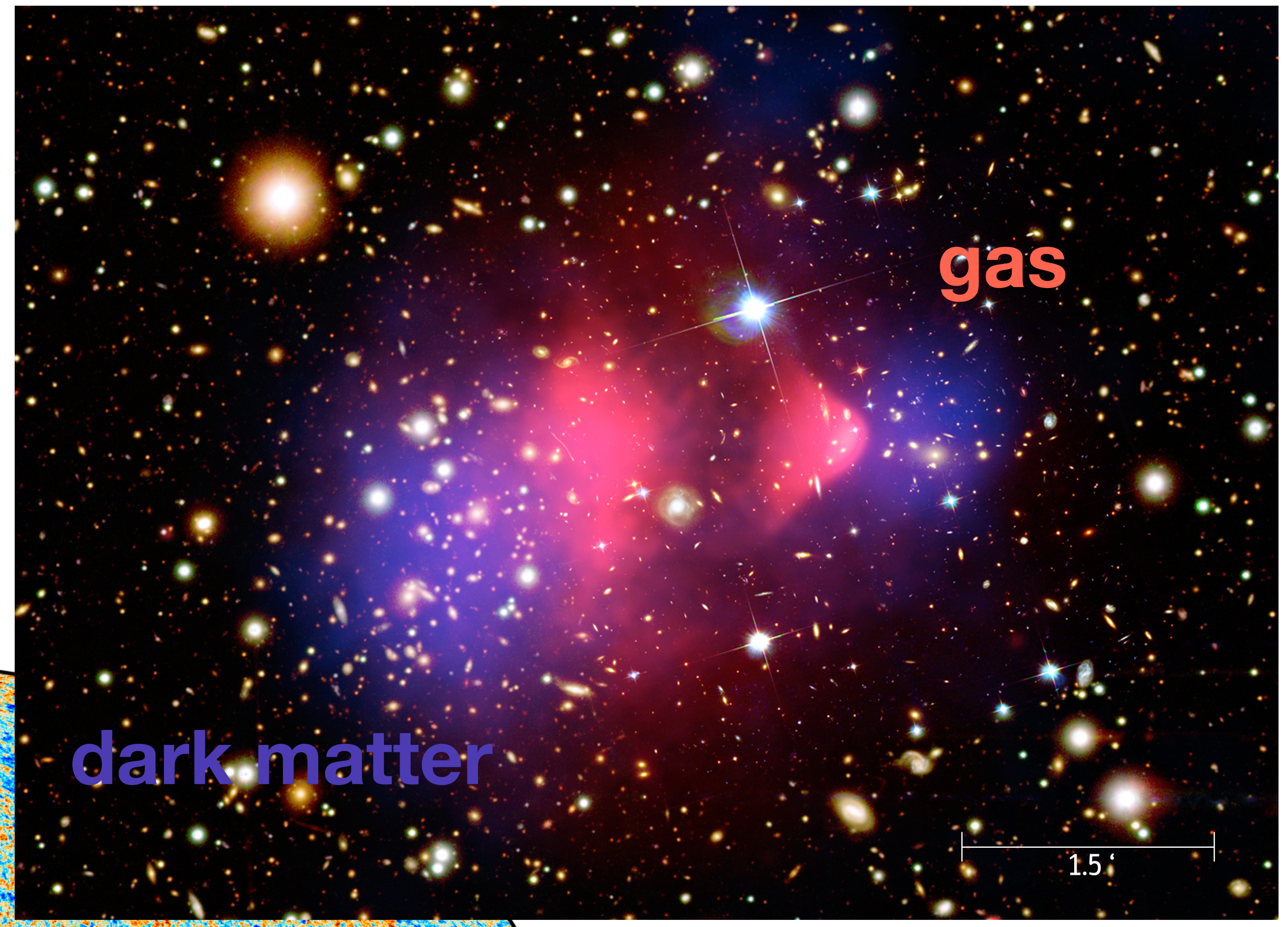

[ESA Spec.Publ. 604 (2006) 723]

but: results are based only on gravitational effects

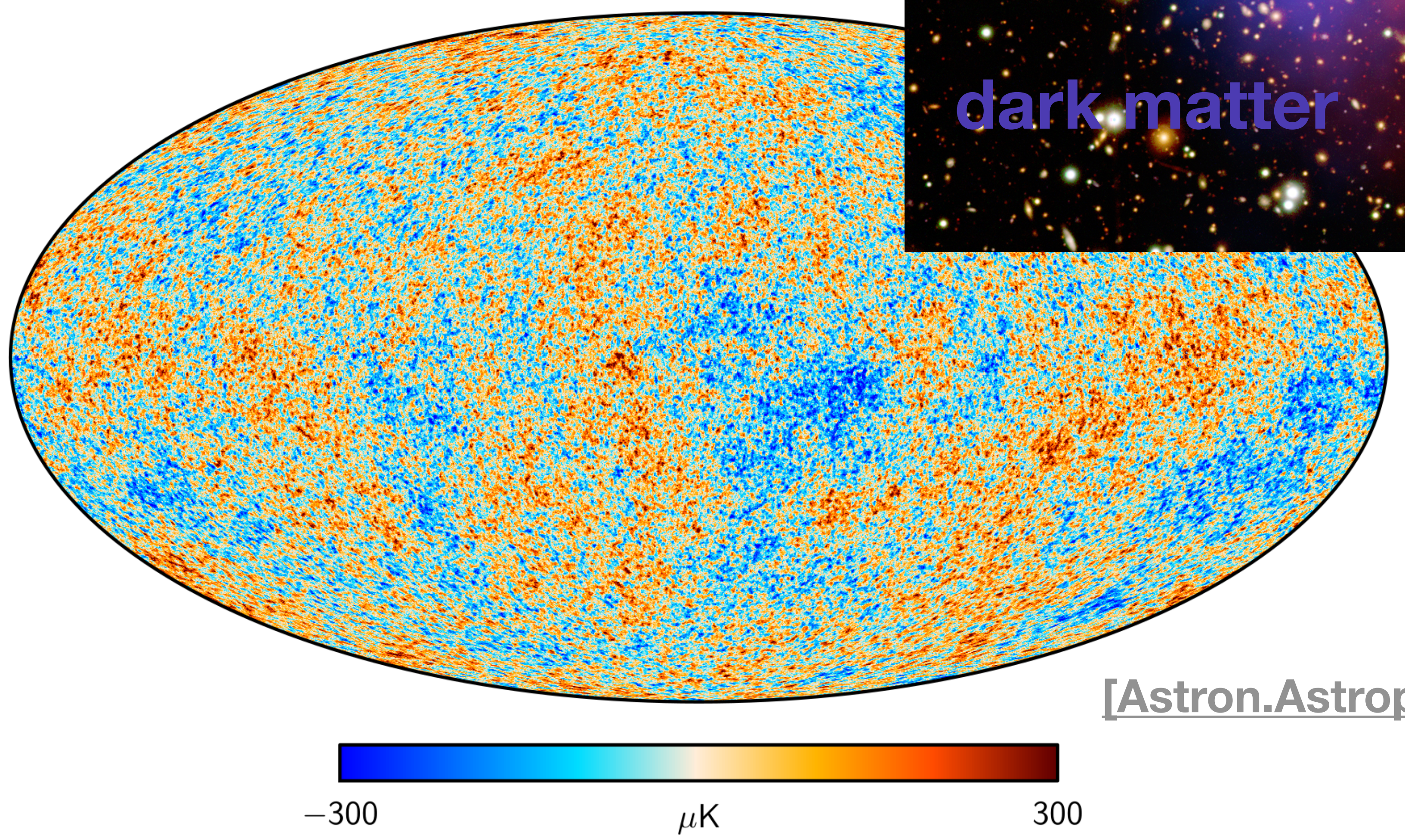

[Astron.Astrophys. 641 (2020) A4]

↠ What is the fundamental nature of DM?

**) based on General Relativity being the correct description of the gravitational interaction on large scales*

Searching for particle DM

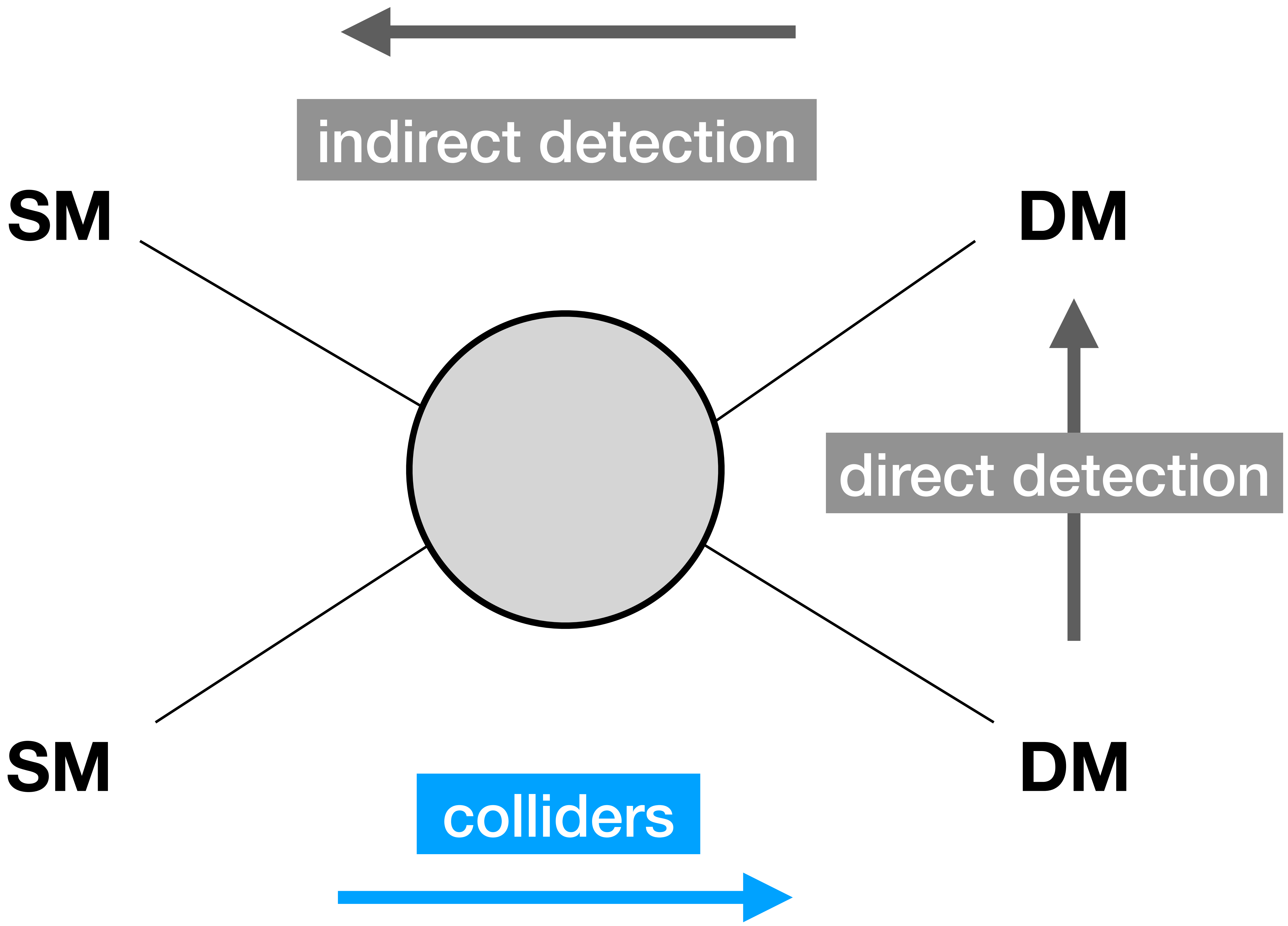

Three *complementary* strategies to search for dark matter particles in the laboratory

*(**if** the SM and the dark sector interact more than gravitationally)*

<u>At colliders</u>:

possibility to *create* dark matter particles if kinematically accessible

DM particles leave no observable signals in the detector

↠ ***missing transverse momentum*** *signatures*

E_T^{miss} reconstruction

➡ DM particles escape detection

➡ momentum imbalance in transverse plane

$$E_{x(y)}^{miss} = -\sum_{i \in \textbf{hard objects}} p_{x(y),i} - \sum_{j \in \textbf{soft signals}} p_{x(y),j} \qquad *)$$

$$\mathbf{E}_T^{miss} = (E_x^{miss}, E_y^{miss})$$

$$E_T^{miss} = |\mathbf{E}_T^{miss}|$$

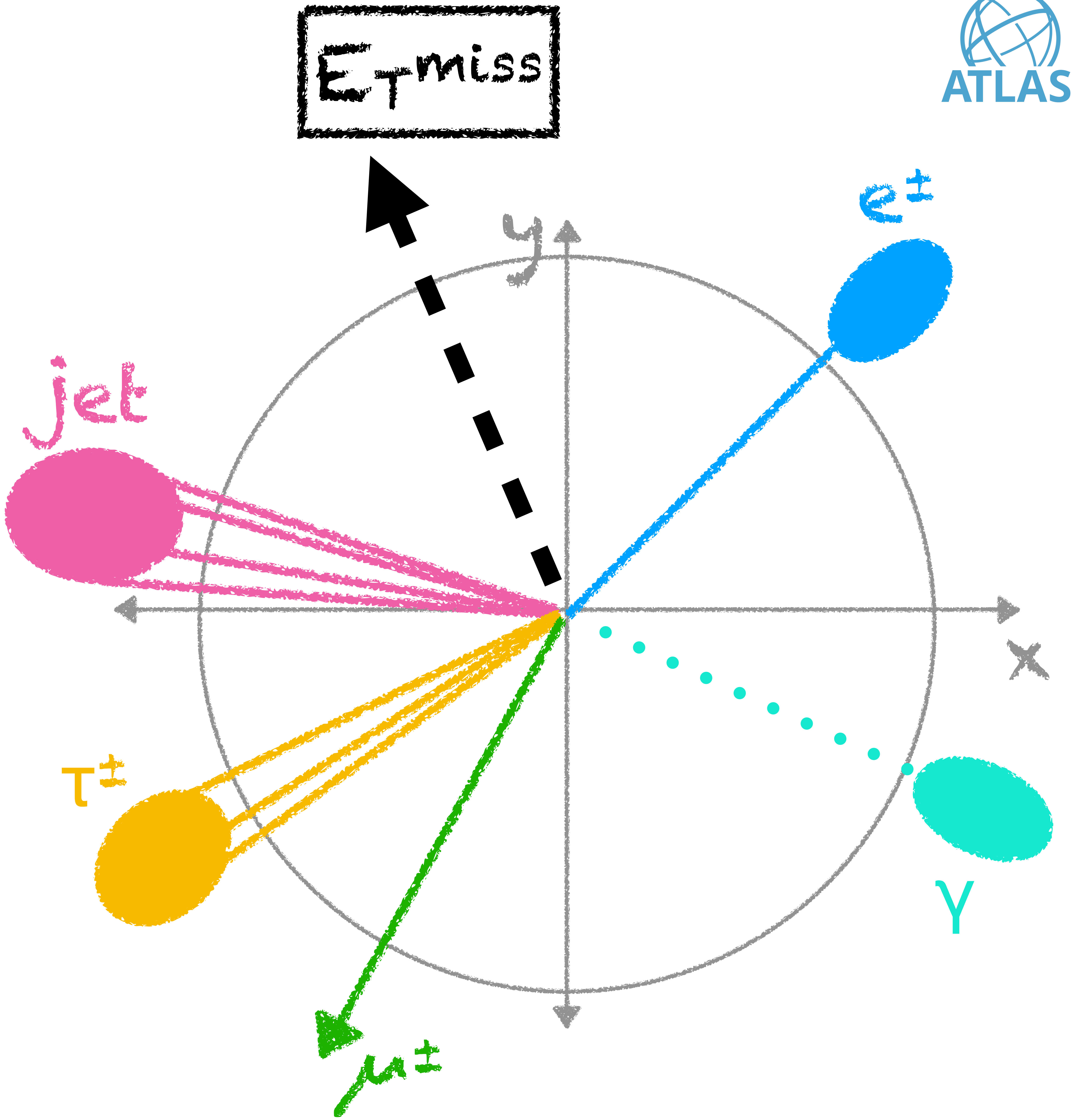

*) negative vector sum of the momenta of all reconstructed **hard objects** (jets, electrons, photons, muons, taus) in an event + **soft term** (tracks that are associated to the primary vertex but none of the hard objects)

Higgs connecting the SM with the dark sector

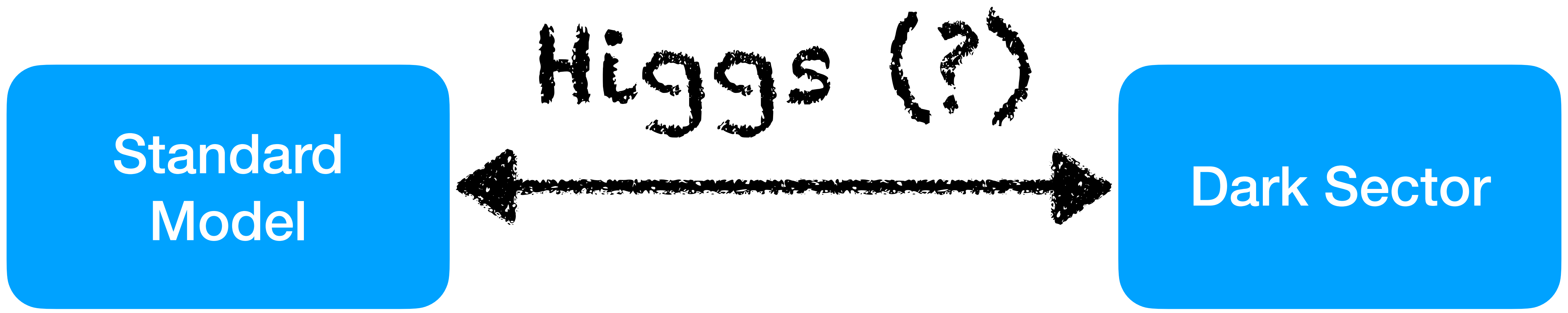

Connection between the SM and the dark sector via the Higgs sector proposed by many models, two possibilities discussed today:

- extended Higgs sector portal models ↠ *DM production in association with a Higgs boson*
- Higgs portal models ↠ *invisible Higgs decays*

Extended Higgs sector portal models

- DM production in association with a Higgs boson

Benchmark simplified model used is **“2HDM+a”**
(see e.g. [Phys.Dark Univ. 27 (2020) 100351])

Based on Type-II Two-Higgs-doublet model (**h**, **H⁰**, **H±**, **A**) + additional pseudoscalar (**a**)

Different signatures can be compared (& combined)

↠ two production modes, that have influence on the kinematics:
ggF (low tanβ) and bbA (high tanβ)

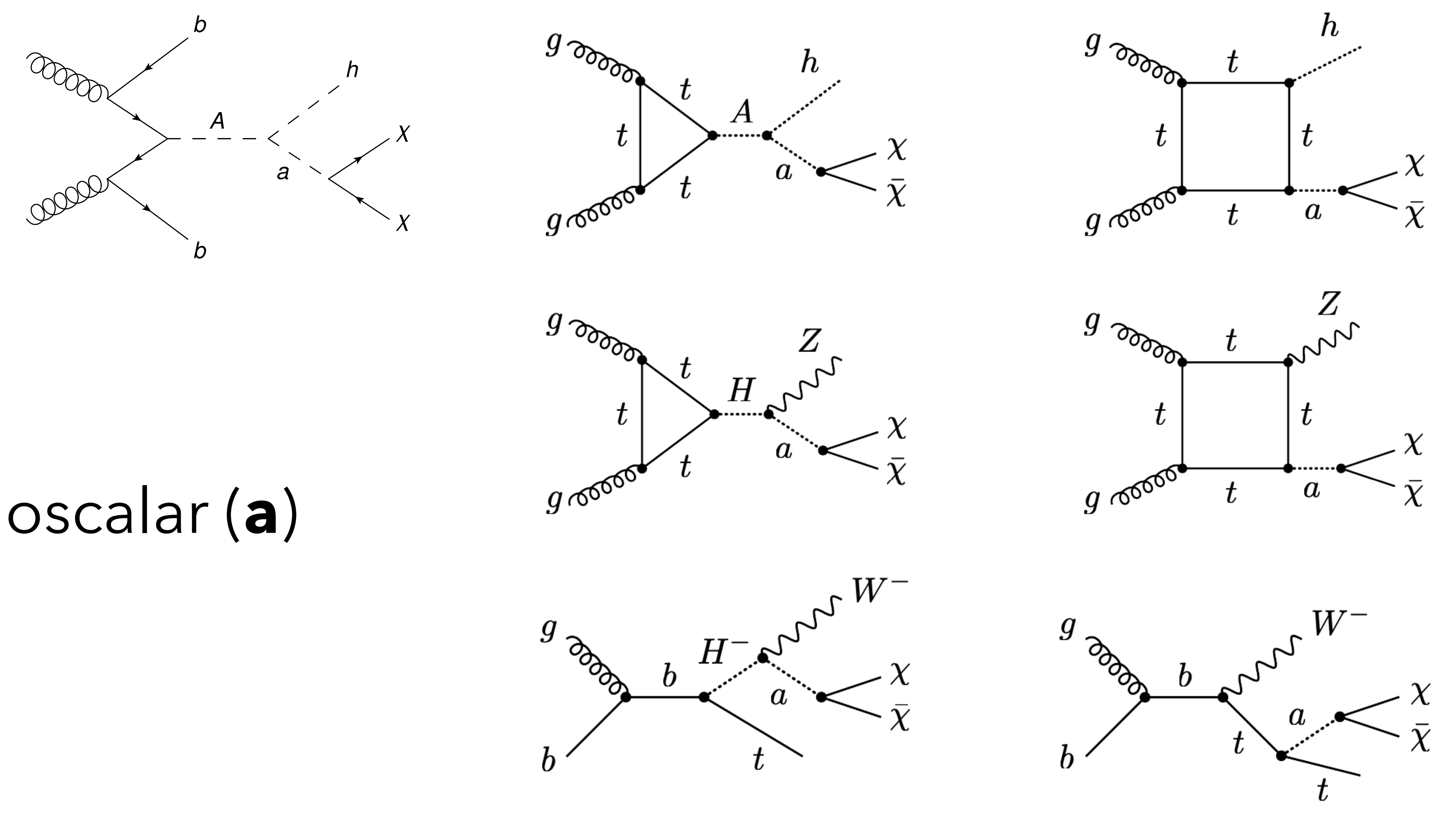

Mono-H

Mono-Z

EW + E_T^{miss}

36fb-1

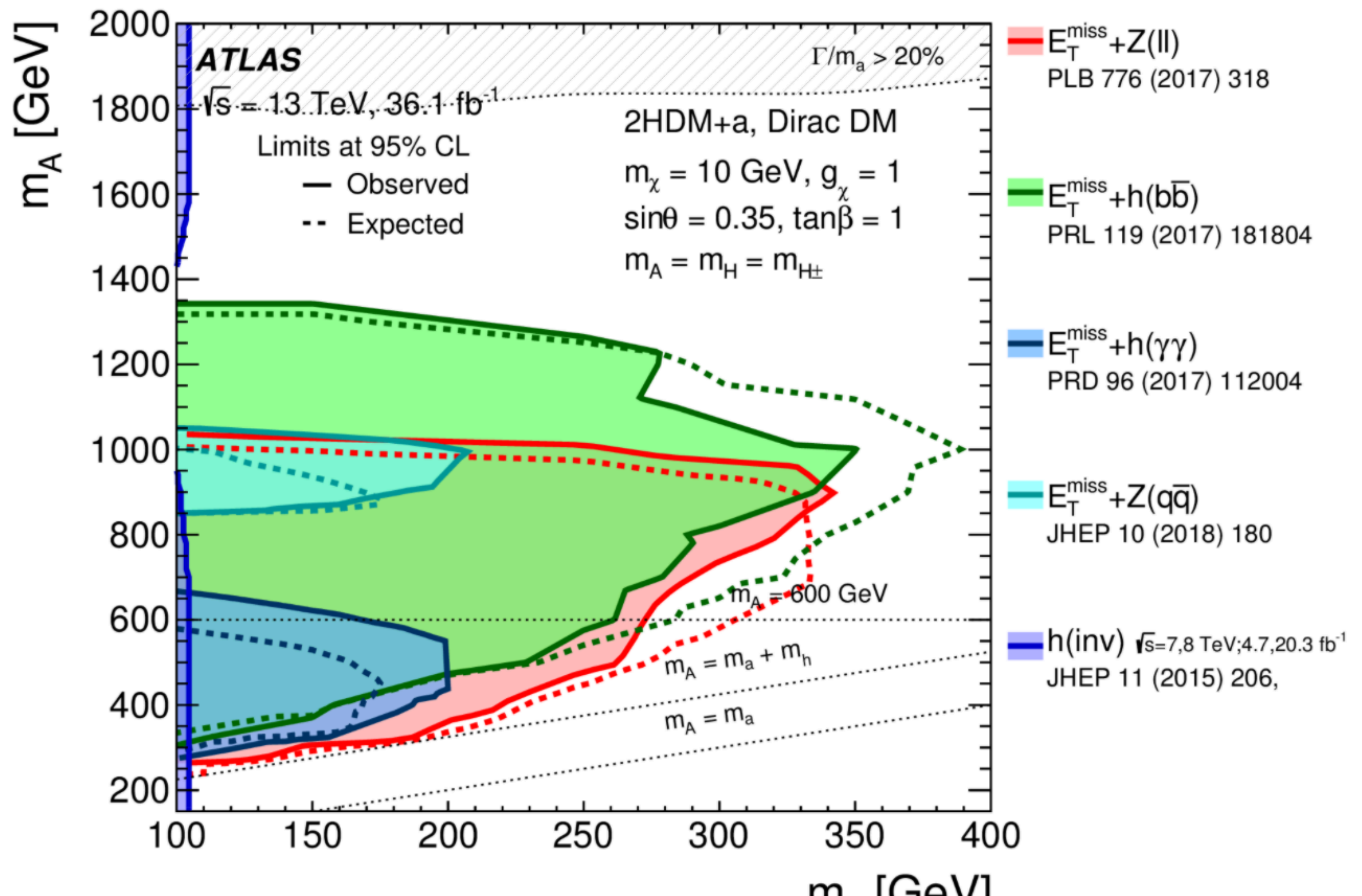

[JHEP 05 (2019) 142]

“Z’2HDM” model

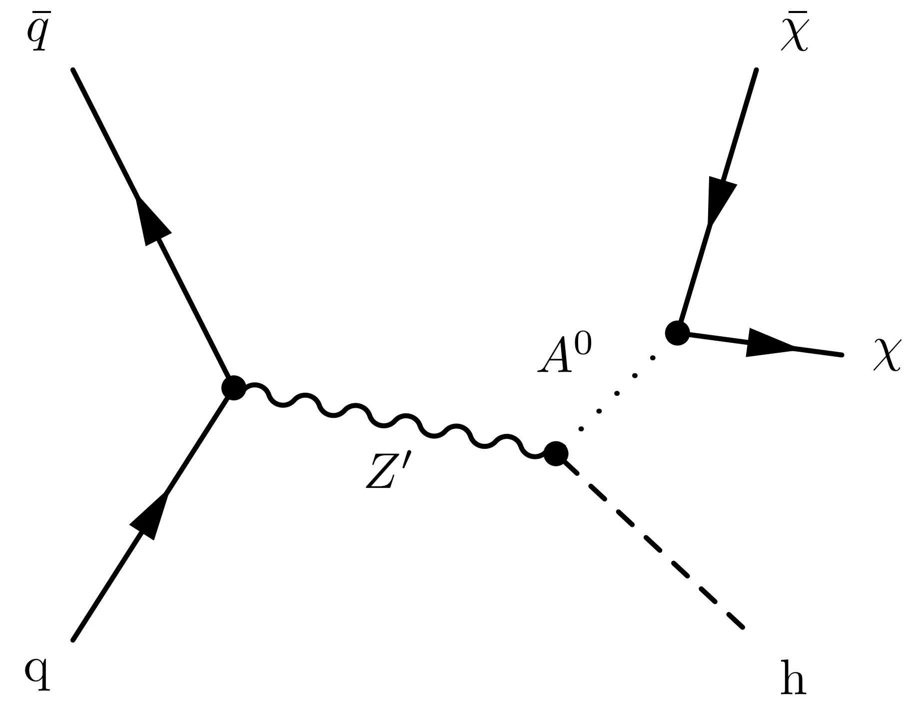

- Extended Higgs sector + new vector mediator
- strongly constrained by dijet searches and B-physics results
- still used as benchmark model, interesting for highly boosted region (high $m_{Z'}$)

Mono-H($b\bar{b}$)

[ATLAS-CONF-2021-006]

Events selected with ≧2 b-tagged jets and E_T^{miss} > 150 GeV

Background rejection (main backgrounds from $t\bar{t}$ and W/Z produced with heavy-flavour jets):

- lepton veto (e±, μ±, τ±) ↞ *reject $\tau^{\pm}$-decays and $W \to \ell\nu$*
- $\Delta\phi(\text{jet}, E_T^{miss}) > 20°$ ↞ *reject fake E_T^{miss} from mismeasurements*

Signal region split into resolved and merged categories, binned in E_T^{miss}

Highly boosted b-jet pair difficult to reconstruct as two jets

↠ *large R jet reconstruction in high E_T^{miss} region*

↠ *within those, b-tagging is done using variable-radius track-jets*

[see e.g. ATLAS-CONF-2018-039]

First result including also a "≧3 b-tag" category for better sensitivity at high tanβ

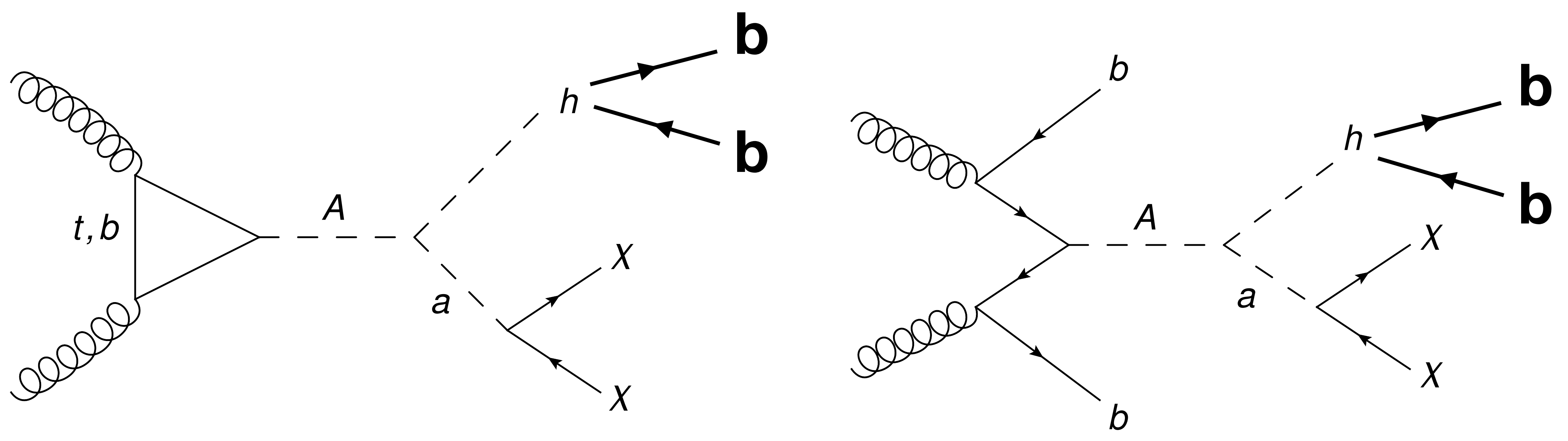

[ATLAS-CONF-2021-006]

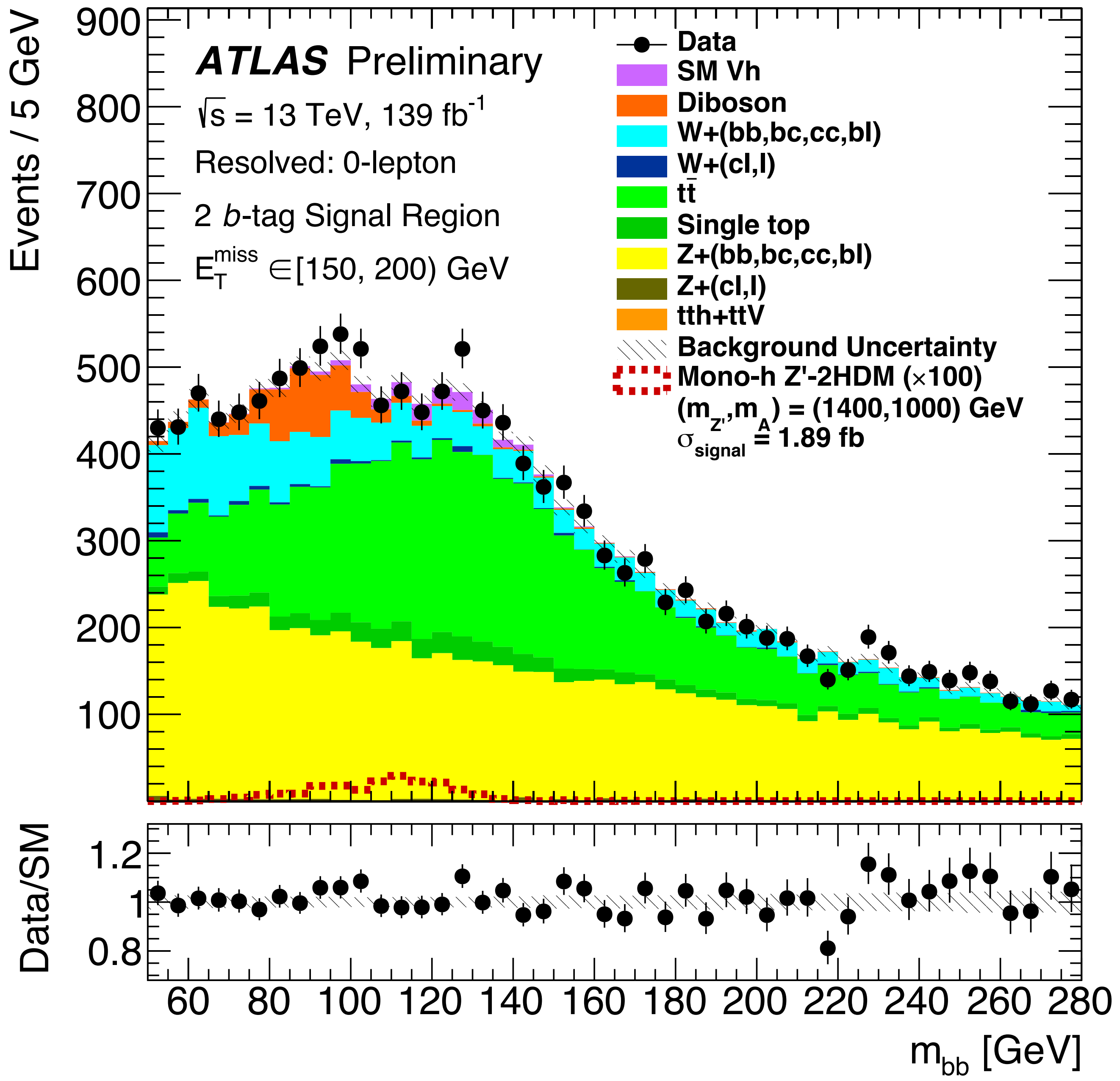

[ATLAS-CONF-2021-006]

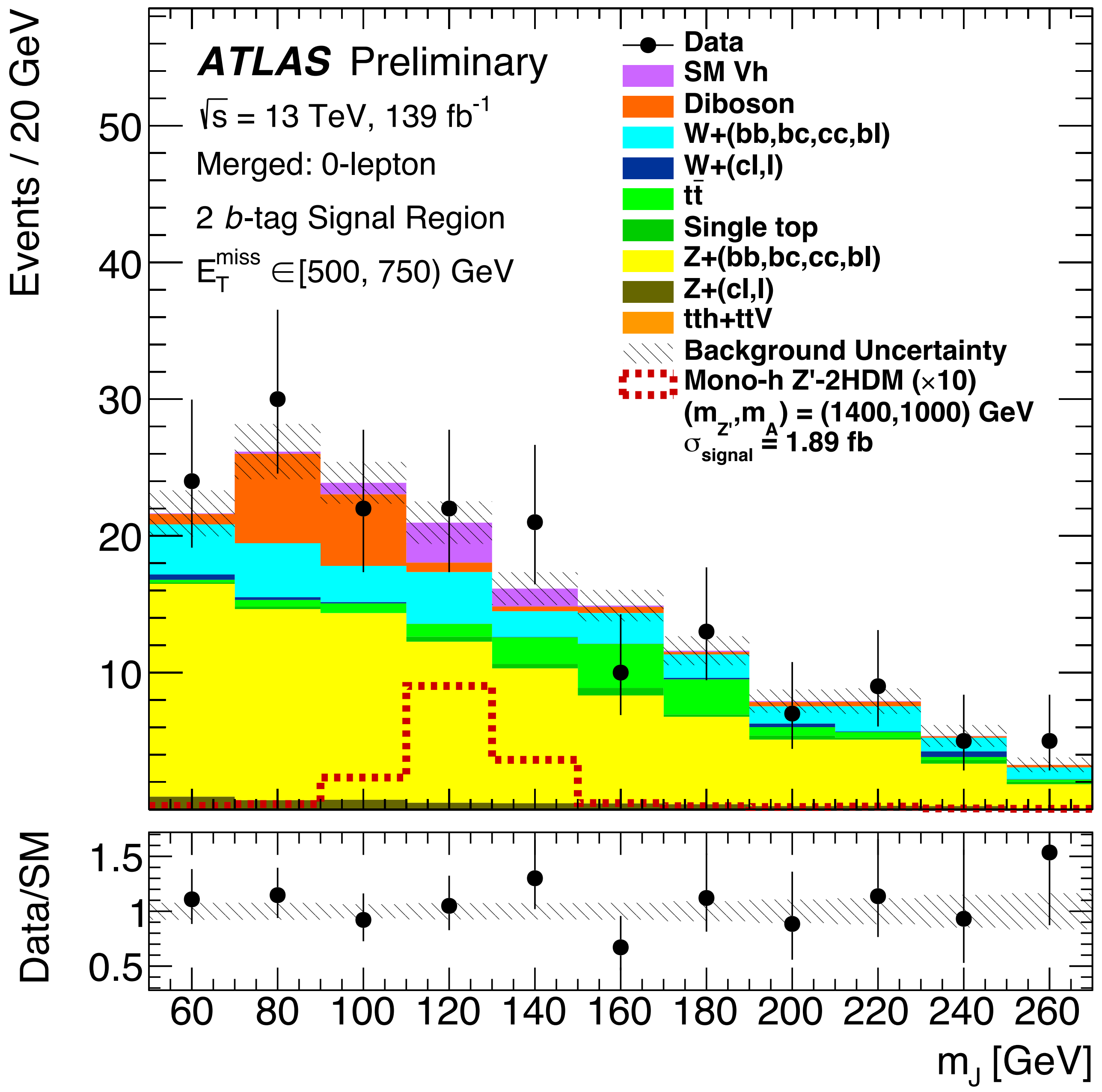

E_T^{miss} < 500 GeV

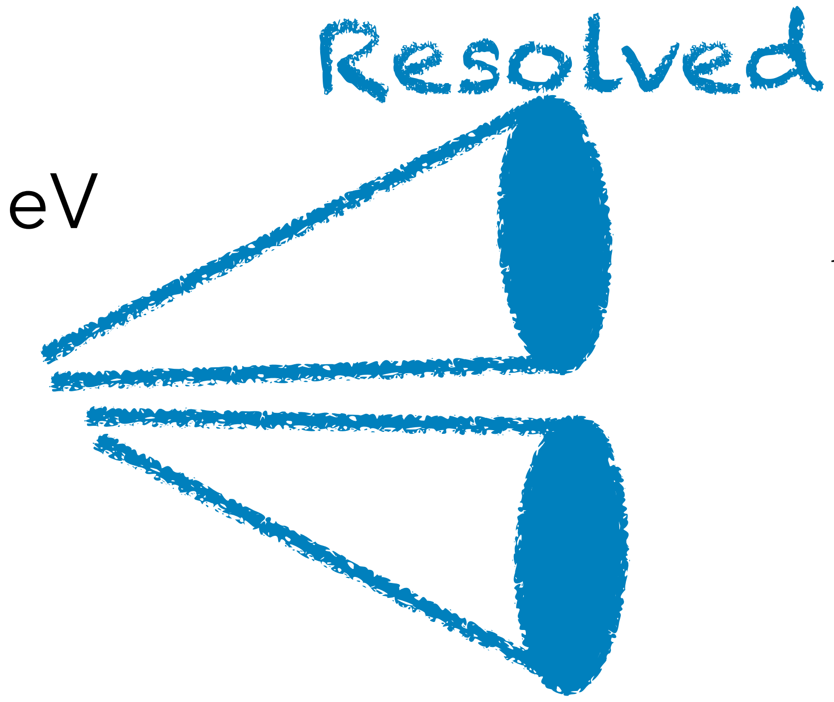

E_T^{miss} > 500 GeV

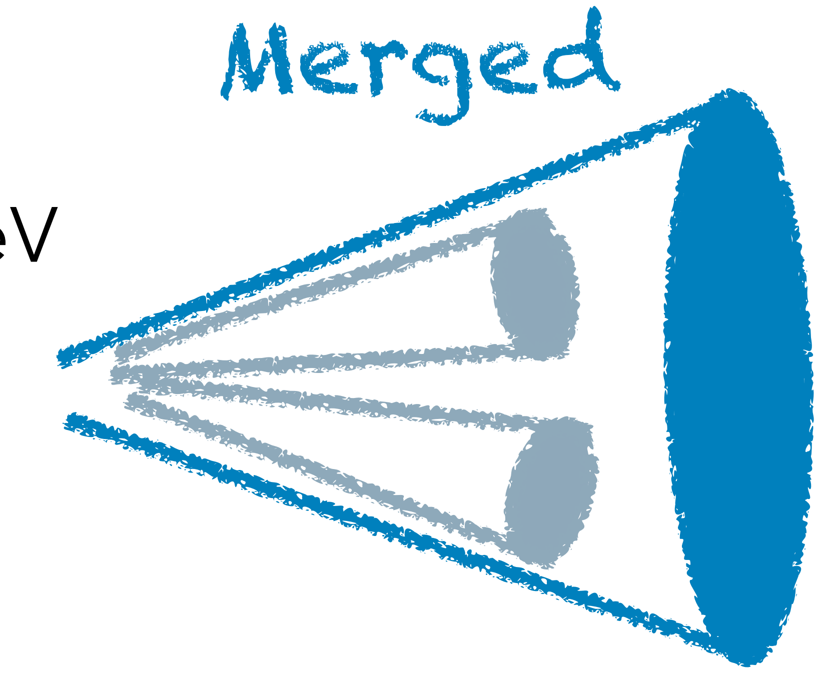

Mono-H($b\bar{b}$) *result*

Simultaneous binned ML fit in the signal and control regions, m_H and E_T^{miss} are the fitted observable in the signal region

Look for an excess of events in the mass spectrum around mH=125 GeV

↠ no significant excess observed, results interpreted as upper limits at 95% CL on the signal cross-section

Z'2HDM

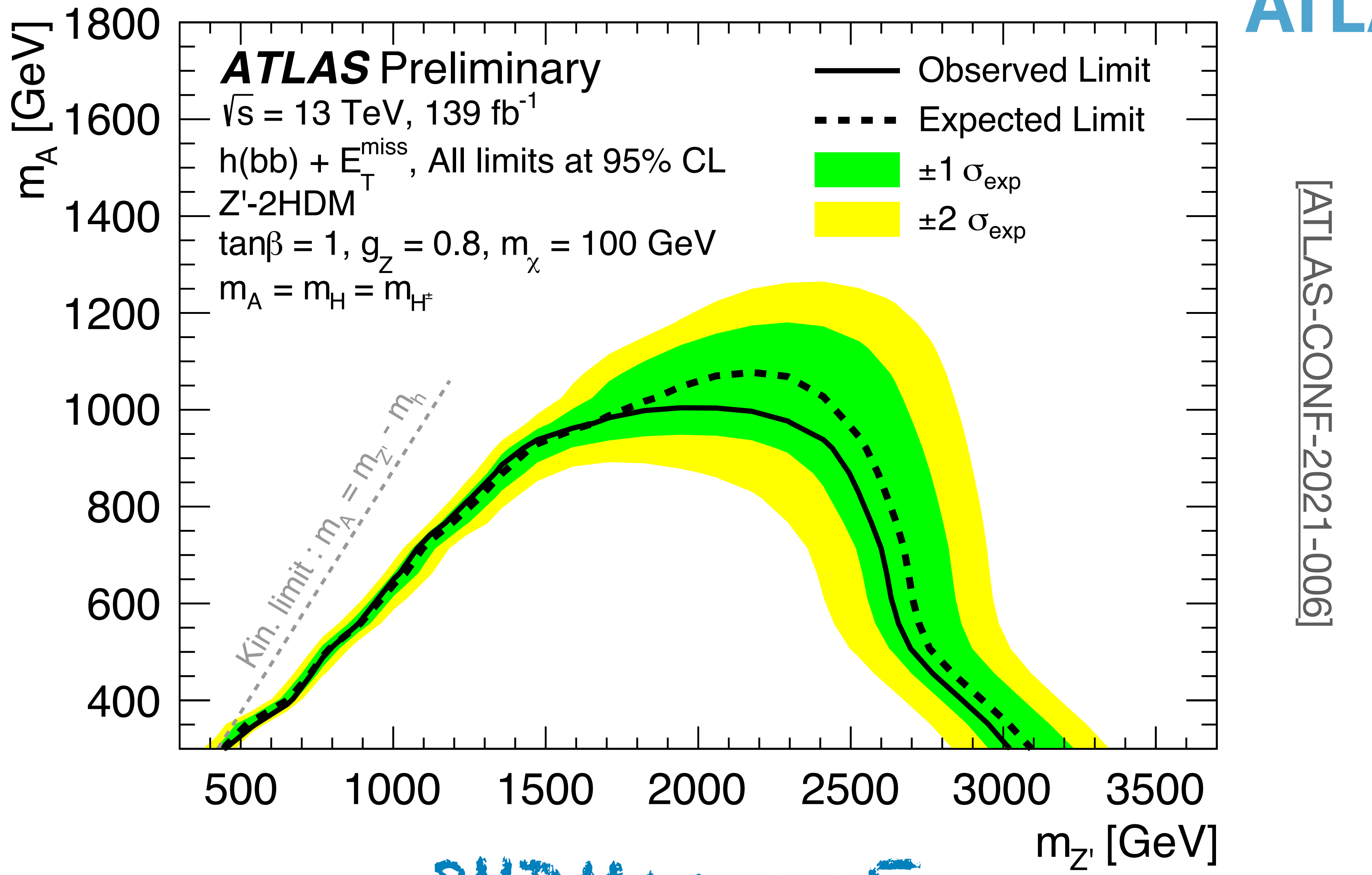

2HDM+a bbA ← first results in this region

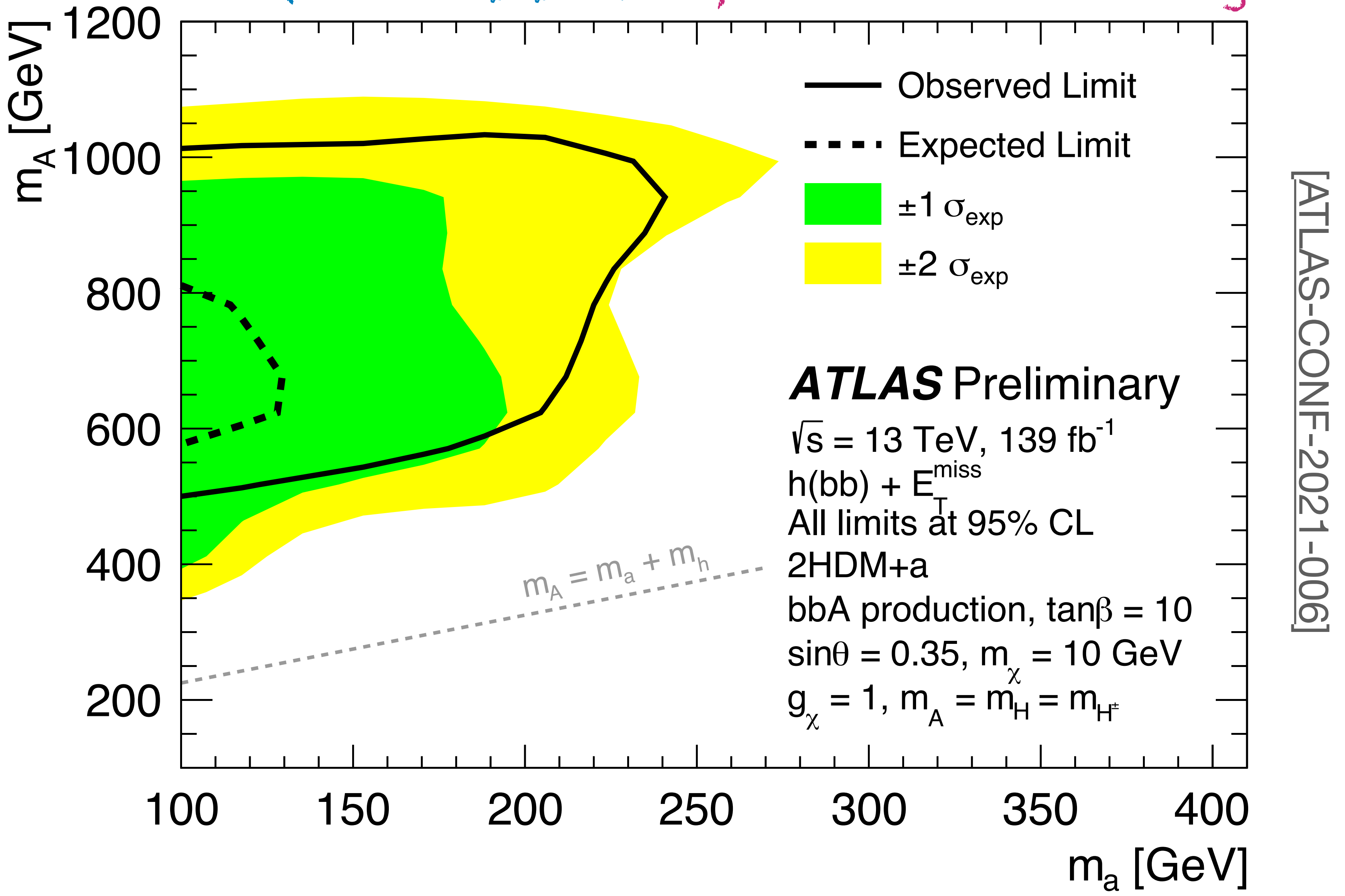

2HDM+a ggF

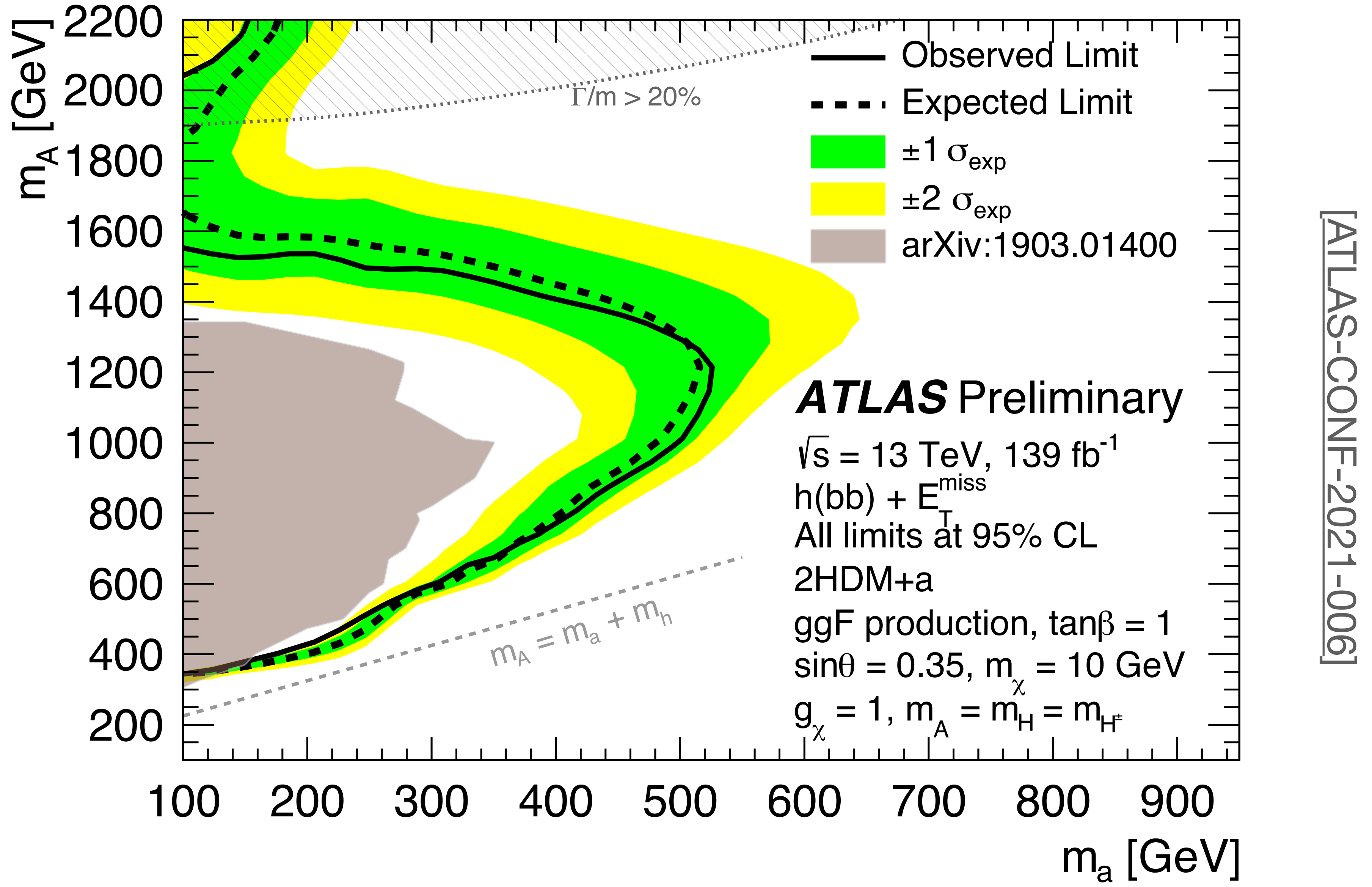

Mono-H($\gamma\gamma$)

[ATLAS-CONF-2020-054]

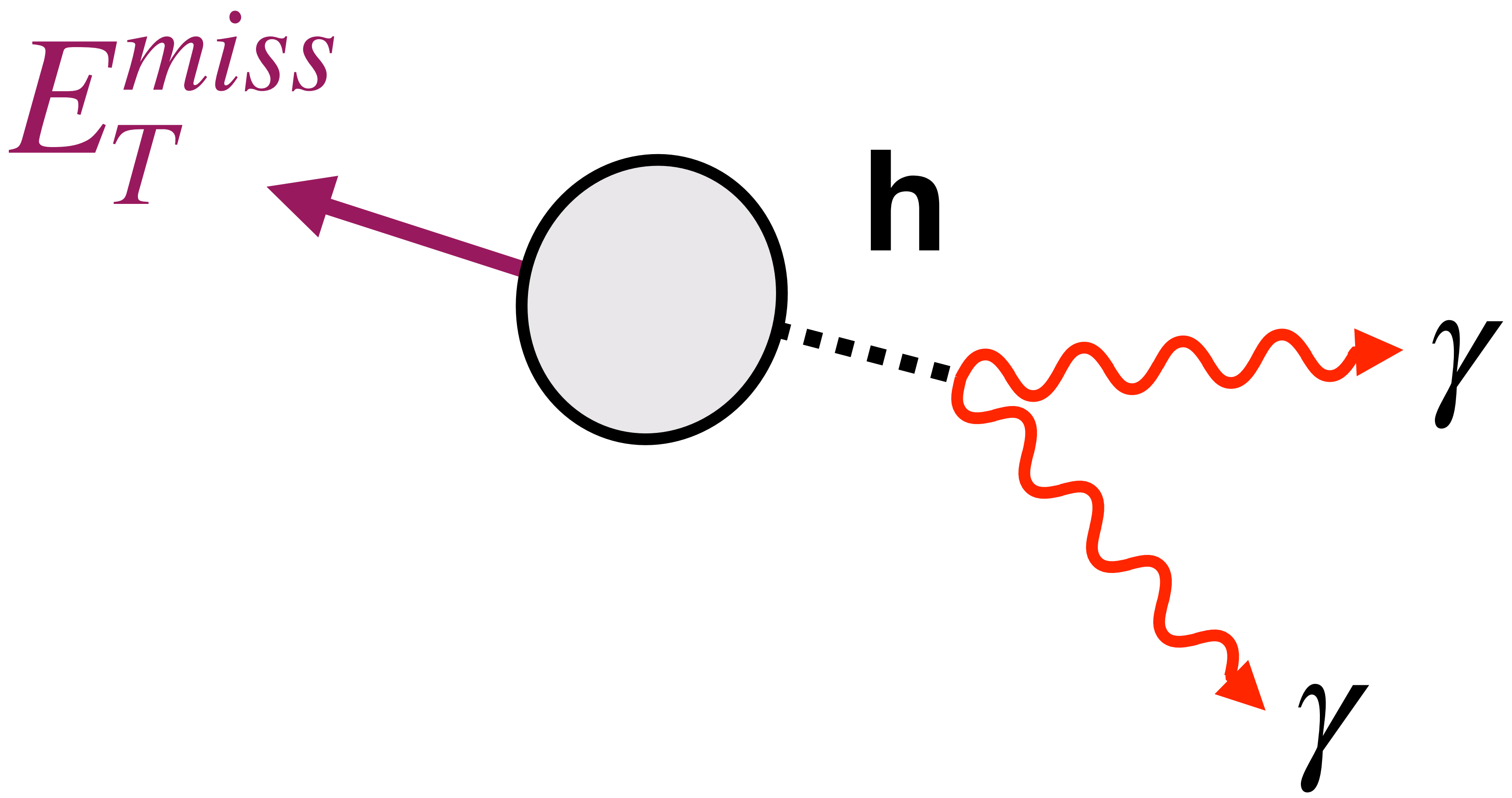

Provides complementarity with $h(\rightarrow b\bar{b}) + E_T^{miss}$ channel

↠ Use of diphoton trigger (instead of E_T^{miss} trigger) allows for **unique sensitivity in the low E_T^{miss}** range (<150 GeV)

Events required to contain:

- 2 photons $105 \leq m_{\gamma\gamma} \leq 160$ GeV
- $E_T^{miss} > 90$ GeV

↞ *all objects reconstructed w.r.t. the vertex selected based on directional information of the photons*

Background rejection cuts:

- E_T^{miss}(diphoton VX) − E_T^{miss}(hardest VX) < 30 GeV
  ↞ *reject fake E_T^{miss} from incorrect jet-vertex association*
- electron & muon veto ↞ *reject $V\gamma$ and $V\gamma\gamma$ backgrounds*

Categorisation performed with BDT, using 2 input variables:

- $S_{E_{\mathrm{T}}^{\mathrm{miss}}} = E_{\mathrm{T}}^{\mathrm{miss}} / \sqrt{\sum E_{\mathrm{T}}}$
- $p_{\mathrm{T}}^{\gamma\gamma}$

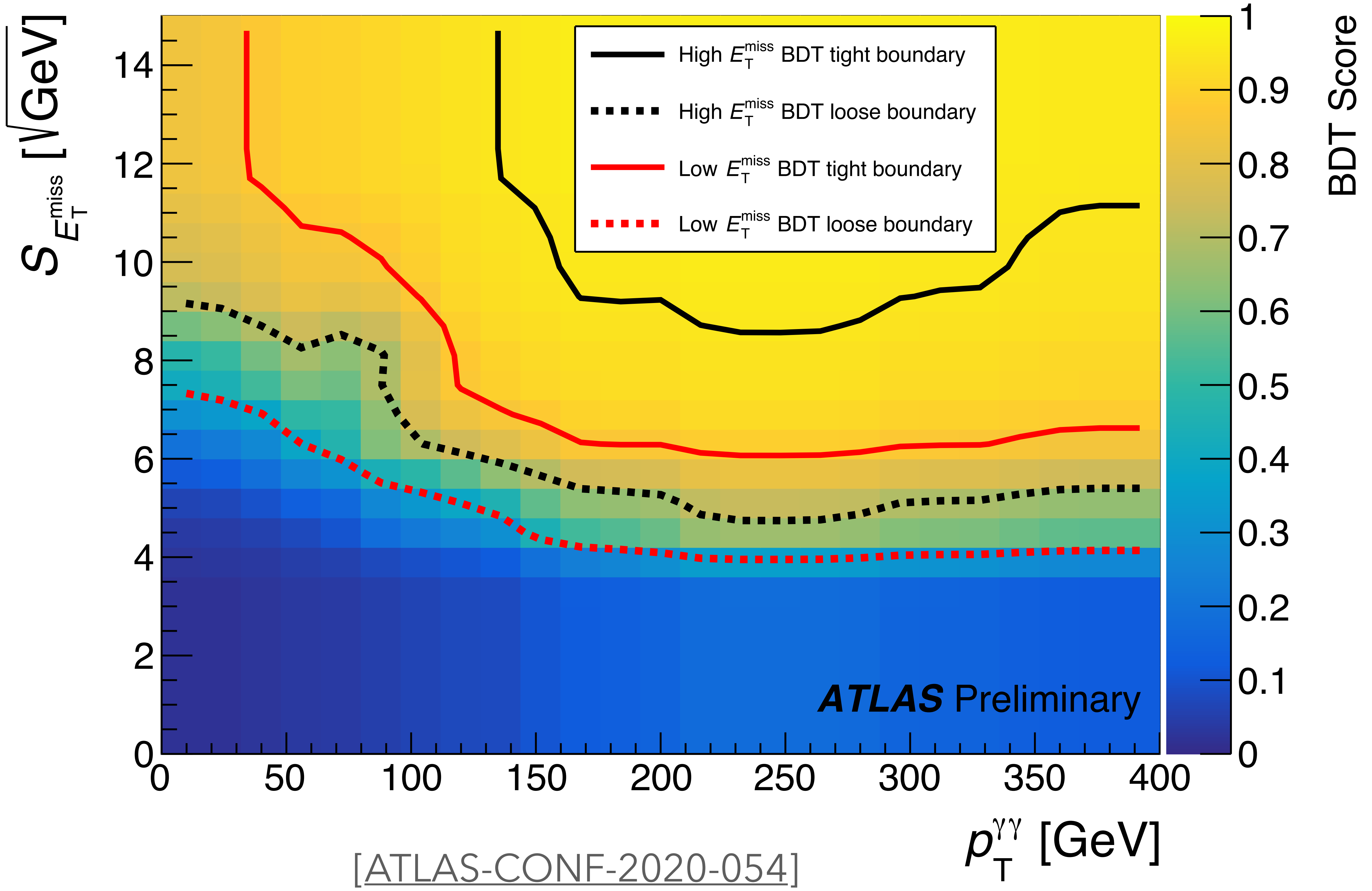

[ATLAS-CONF-2020-054]

Mono-H($\gamma\gamma$) *result*

Shape analysis: **unbinned** fit on the invariant diphoton mass $m_{\gamma\gamma}$ performed simultaneously in all 4 signal categories

"SM Higgs" peak and signal: $m_{\gamma\gamma}$ shape modelled with double-sided Crystal Ball function (gaussian core and power laws in the tails)

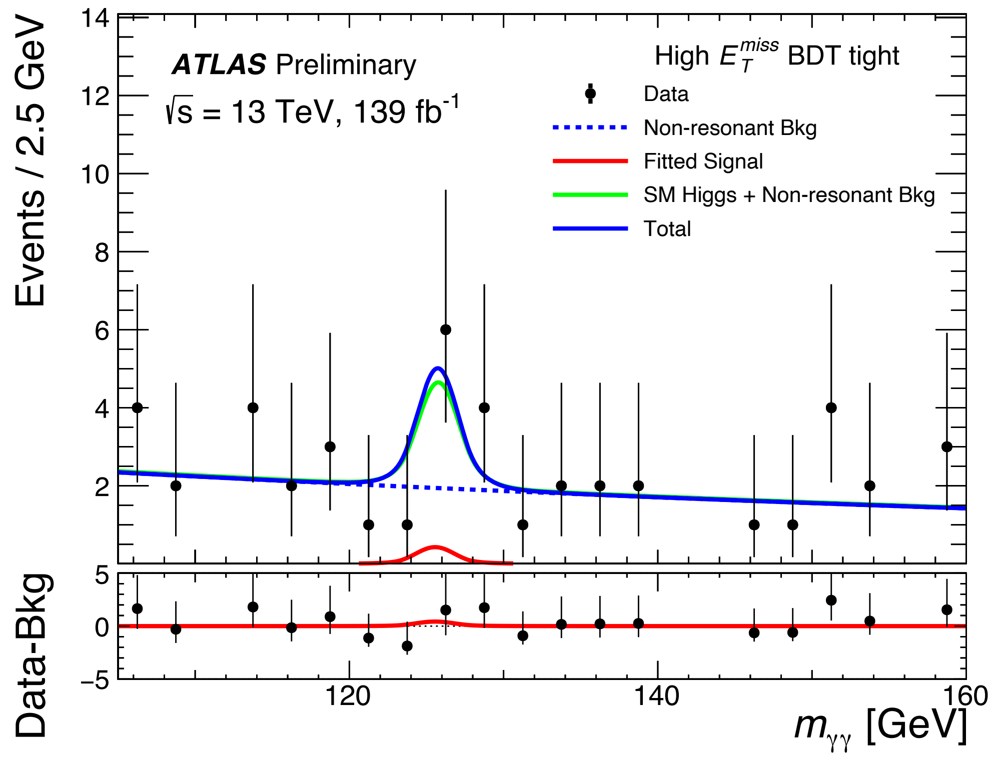

[ATLAS-CONF-2020-054]

Non-resonant BG modelled by smoothly falling function ↠ *functional form based on MC templates, parameters estimated from data*

↠ no significant excess above the SM prediction observed

2HDM+a

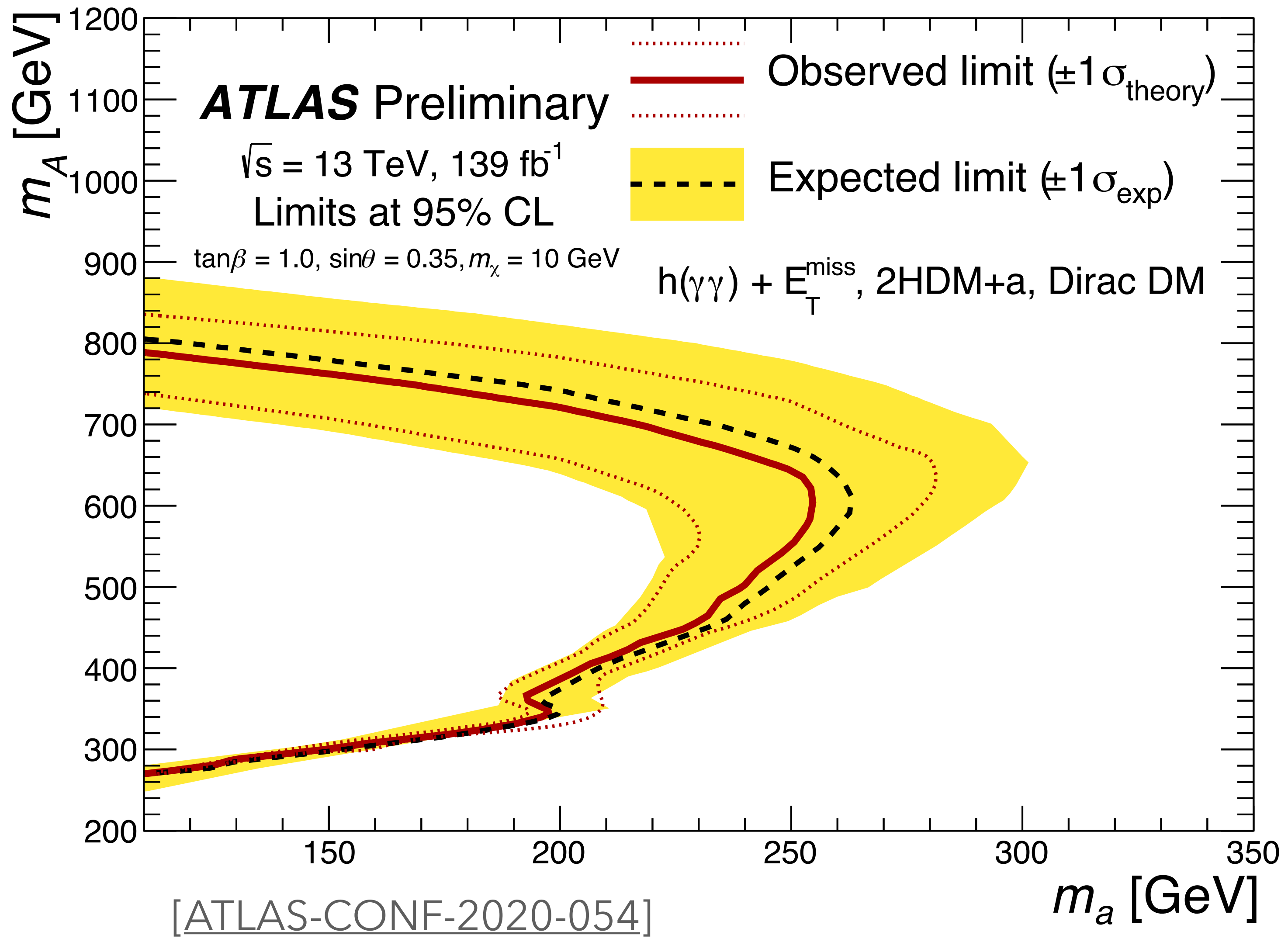

[ATLAS-CONF-2020-054]

Z'2HDM

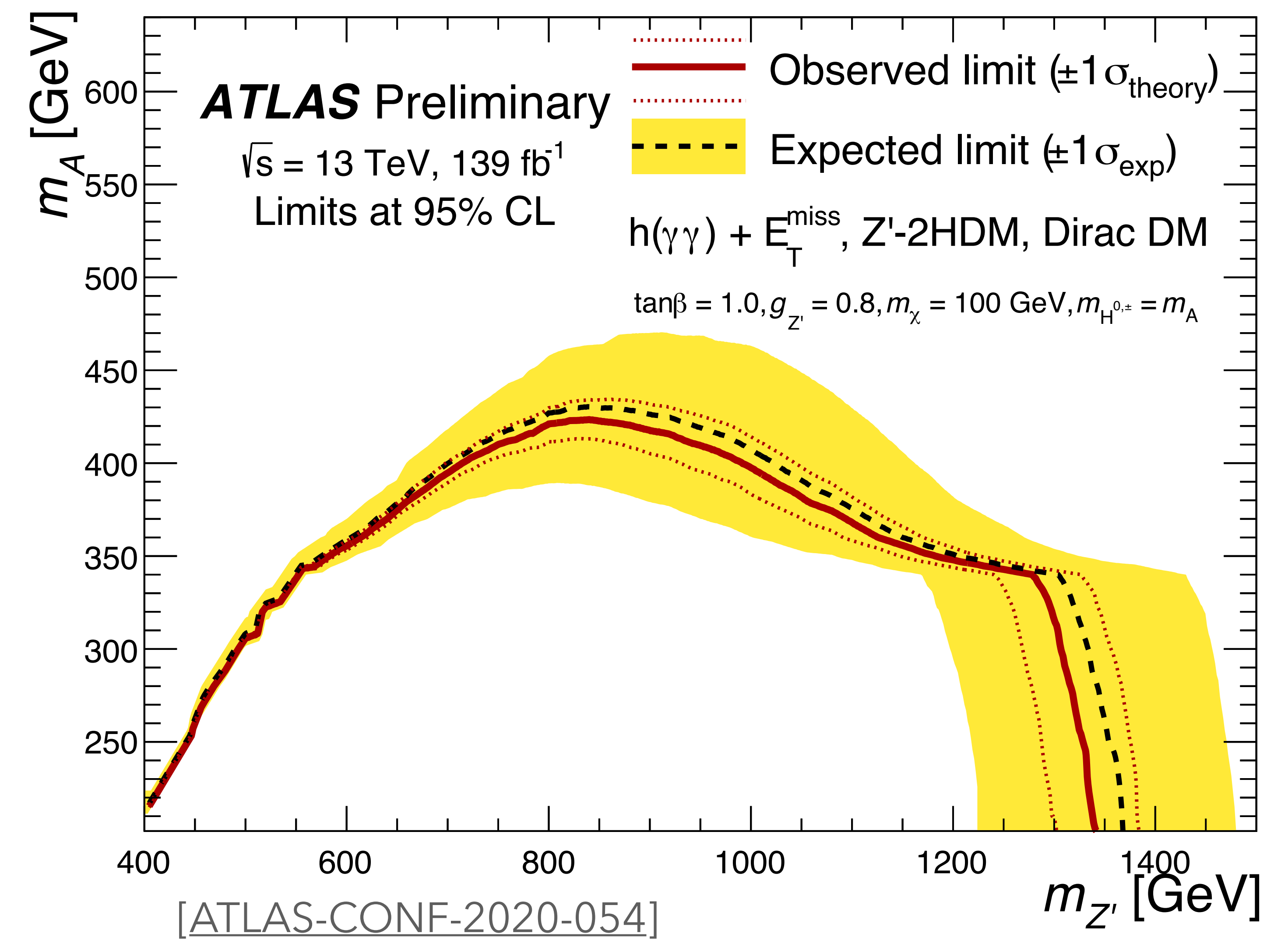

[ATLAS-CONF-2020-054]

ATLAS

Higgs portal: invisible Higgs decays

if $m_\chi \leq m_h/2$, Higgs boson could decay to dark matter particles

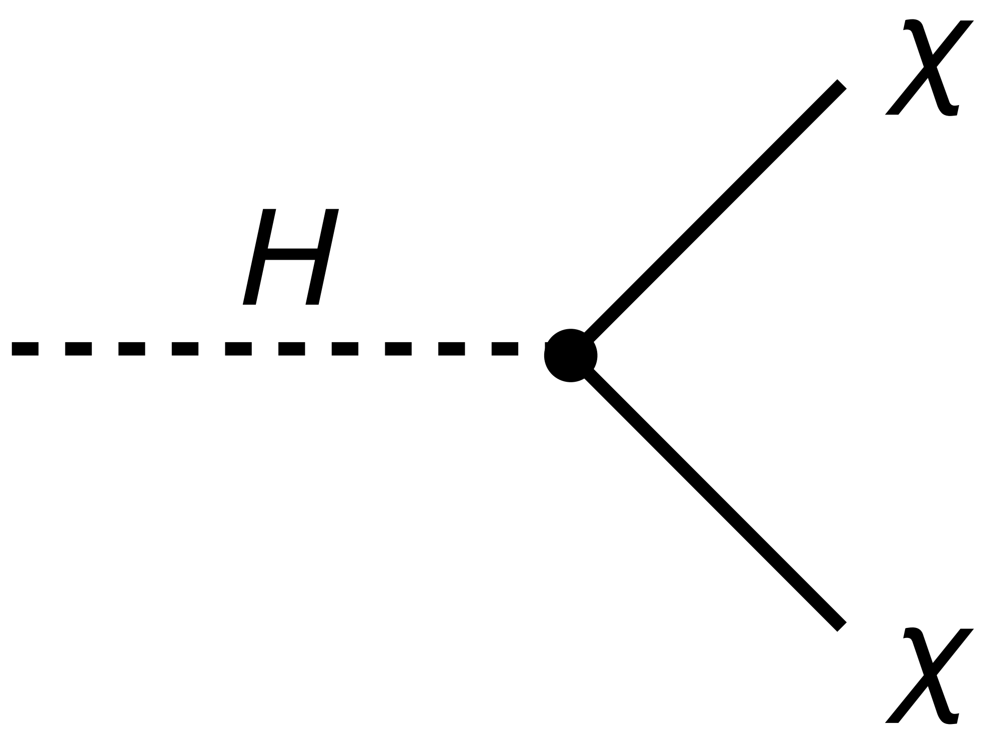

In SM, invisible decay $H \rightarrow ZZ^* \rightarrow 4\nu$ has very small **branching fraction** ~0.12%

BSM models increase the H(inv) branching fraction to up to $\mathcal{O}(10\%)$

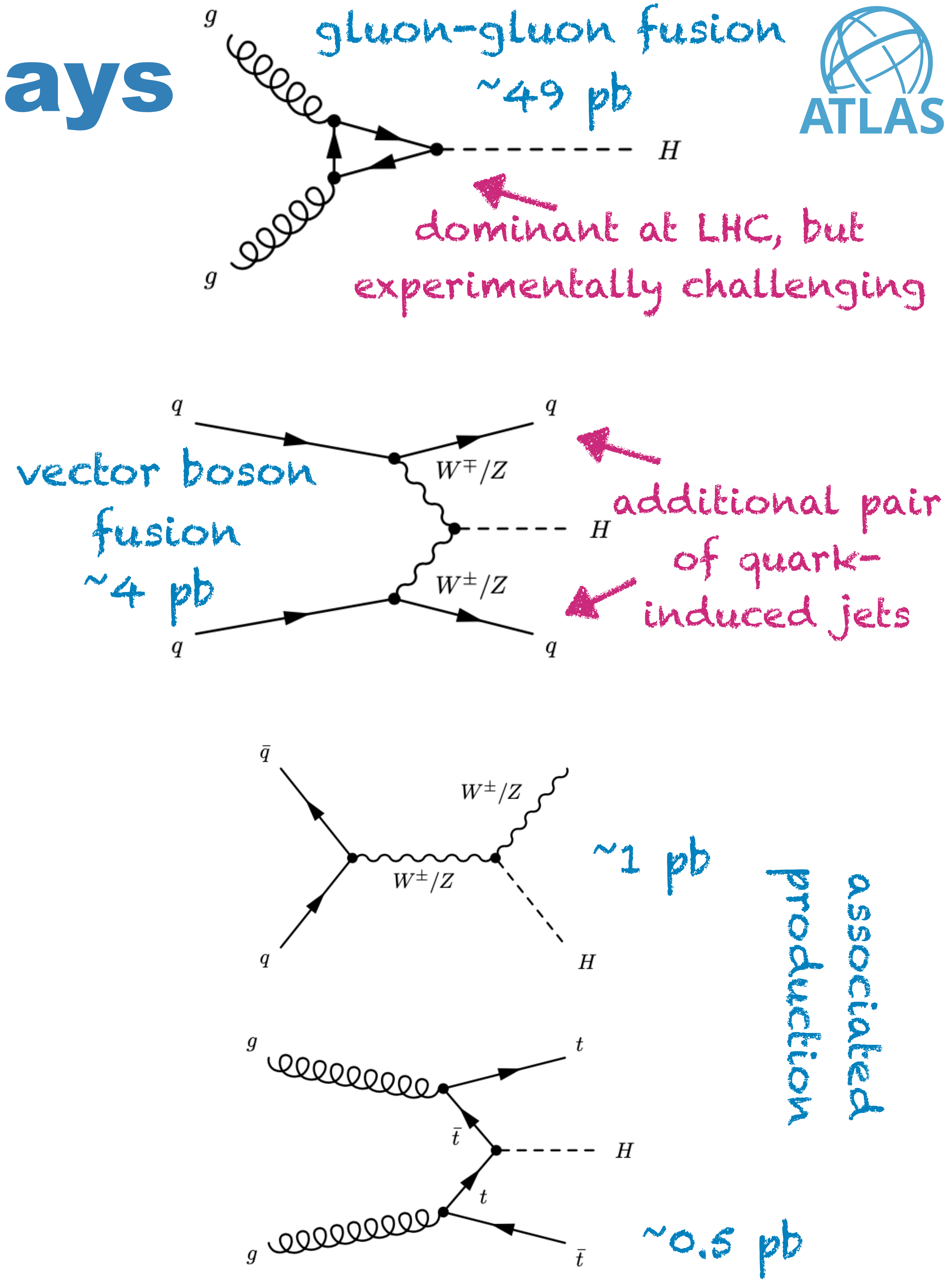

Main Higgs production modes at the LHC

VBF H→inv + photon

[ATLAS-CONF-2021-004]

First search of invisible decay of the Higgs boson through VBF in association with an emitted photon

Improved background rejection and signal reconstruction efficiency compared to typical VBF H(inv) analysis

Dominant background contributions from $Z(\rightarrow \nu\nu)\gamma$+jets and $W(\rightarrow \ell\nu)\gamma$+jets

SM $H \rightarrow Z(\rightarrow \nu\nu)\gamma$ process has same signature as signal, but negligible contribution in the signal regions

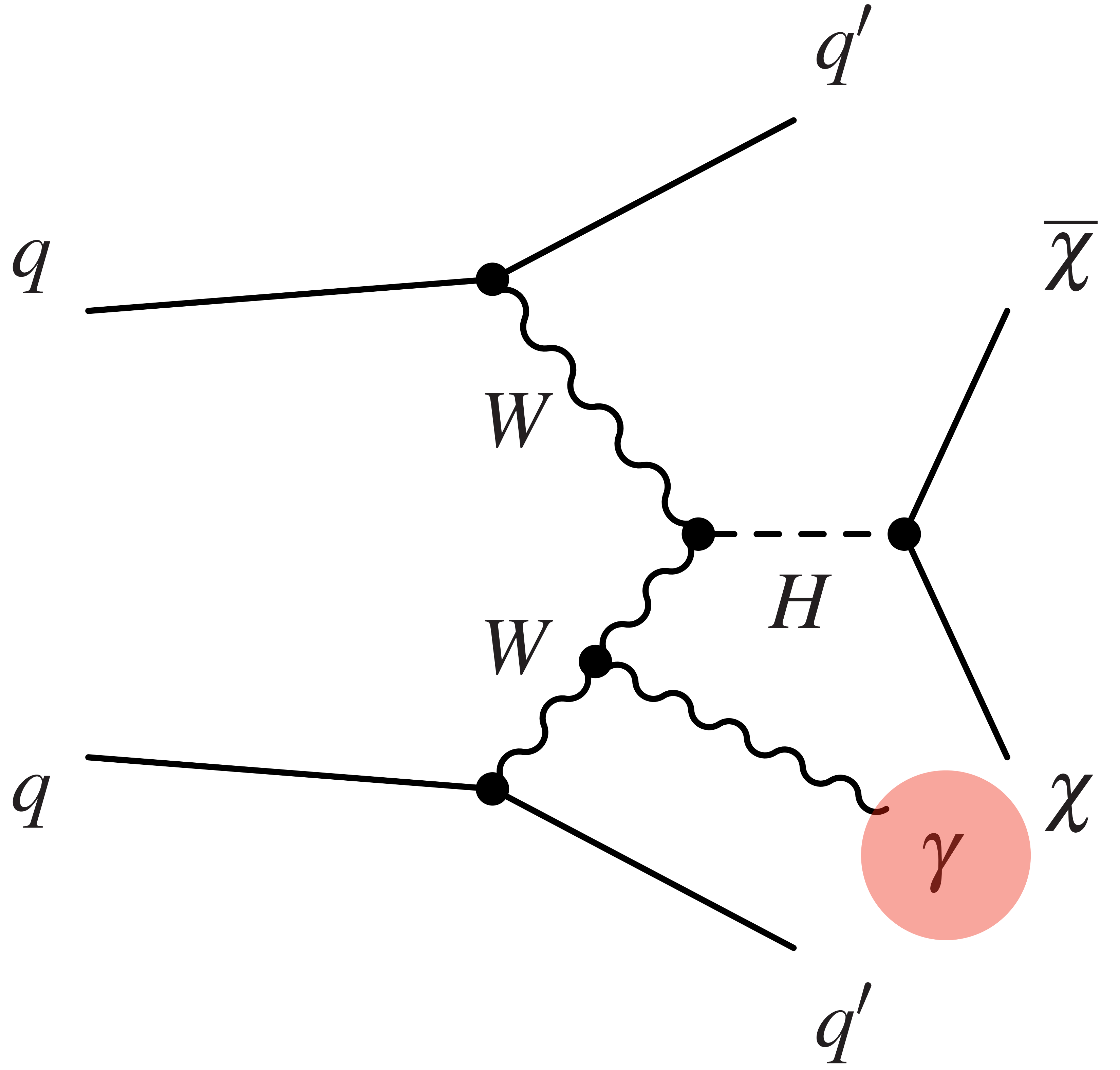

VBF H→inv + photon *analysis strategy & result*

[ATLAS-CONF-2021-004]

Preselection is relaxed compared to the VBF H→inv selection

- large invariant mass $m_{jj} > 0.25$ TeV
- large pseudo-rapidity separation $\Delta\eta_{jj} > 3.0$
- large missing transverse momentum $E_T^{miss} > 150$ GeV

Requires a single photon:

- $15\text{ GeV} < p_T < 110\text{ GeV}$ ↞ *upper threshold reduces γ+jet background*
- $C_\gamma > 0.4$ ↞ *"centrality", 1 if photon is centred between the two jets, 0 if inf. farther forward*

Event classification uses a **dense neural network**, categorised by the output score in 4 bins

Control regions defined to constrain the backgrounds

Observed (expected) upper limit on the H→inv branching fraction:

$BR_{H\to inv} < 0.37\ (0.34^{+0.15}_{-0.10})$

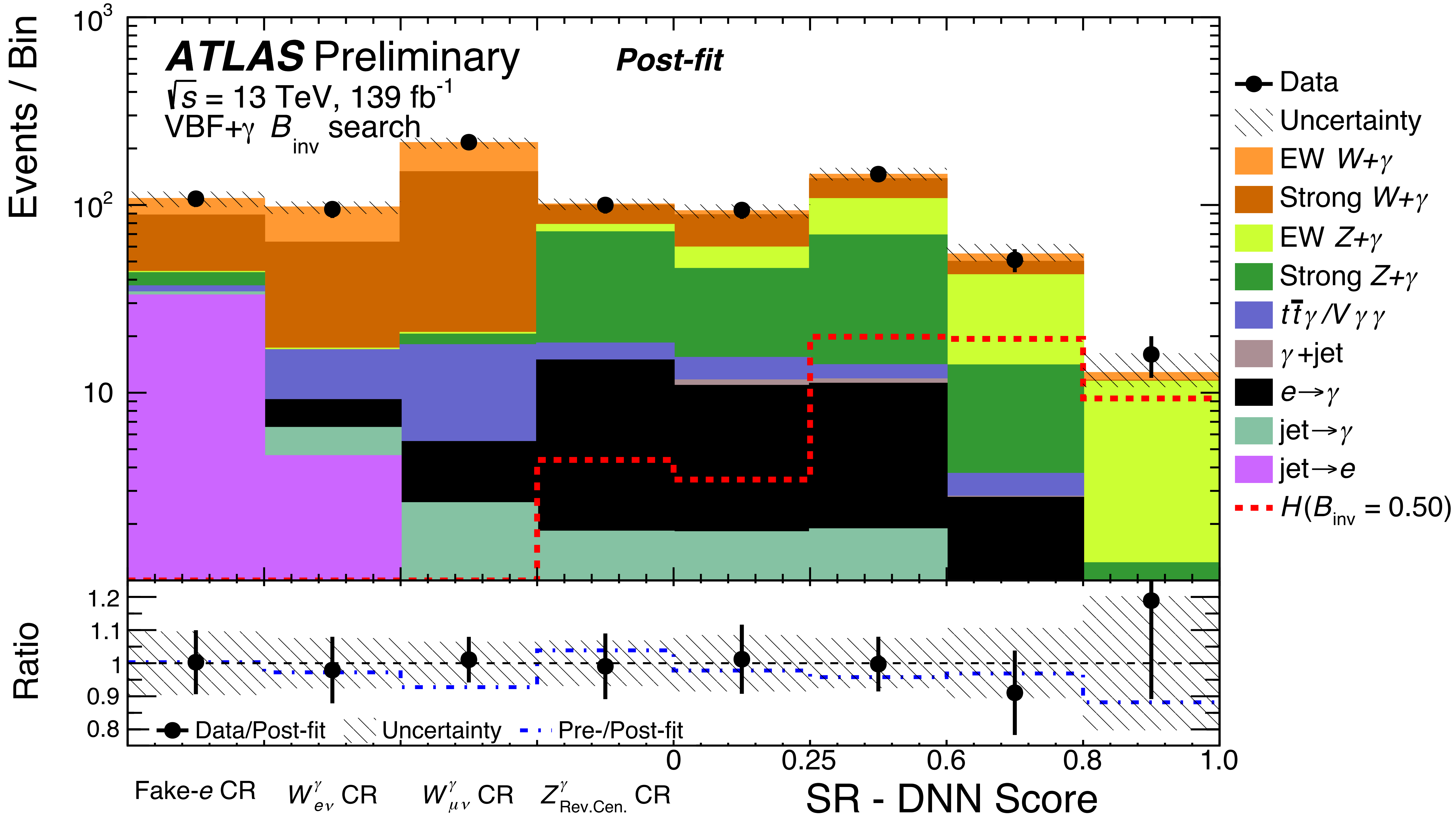

$$C_\gamma = \exp\left(-\frac{4}{(\eta_1-\eta_2)^2}\left(\eta_\gamma - \frac{\eta_1+\eta_2}{2}\right)^2\right)$$

VBF H→inv + photon *dark photon*

Additional $H \to \gamma\gamma_D$ **dark photon** interpretation provided

Dark photon model, coupling with the Higgs boson through a U(1) unbroken dark sector

Different event classification due to the signature in transverse mass defined by E_T^{miss} and the photon

$$m_T(\gamma, E_T^{miss}) = \sqrt{2p_T^{\gamma}E_T^{miss}[1 - \cos(\phi_\gamma - \phi_{E_T^{miss}})]}$$

Low and high m_{jj} bin, different relative contributions of ggF and VBF productions

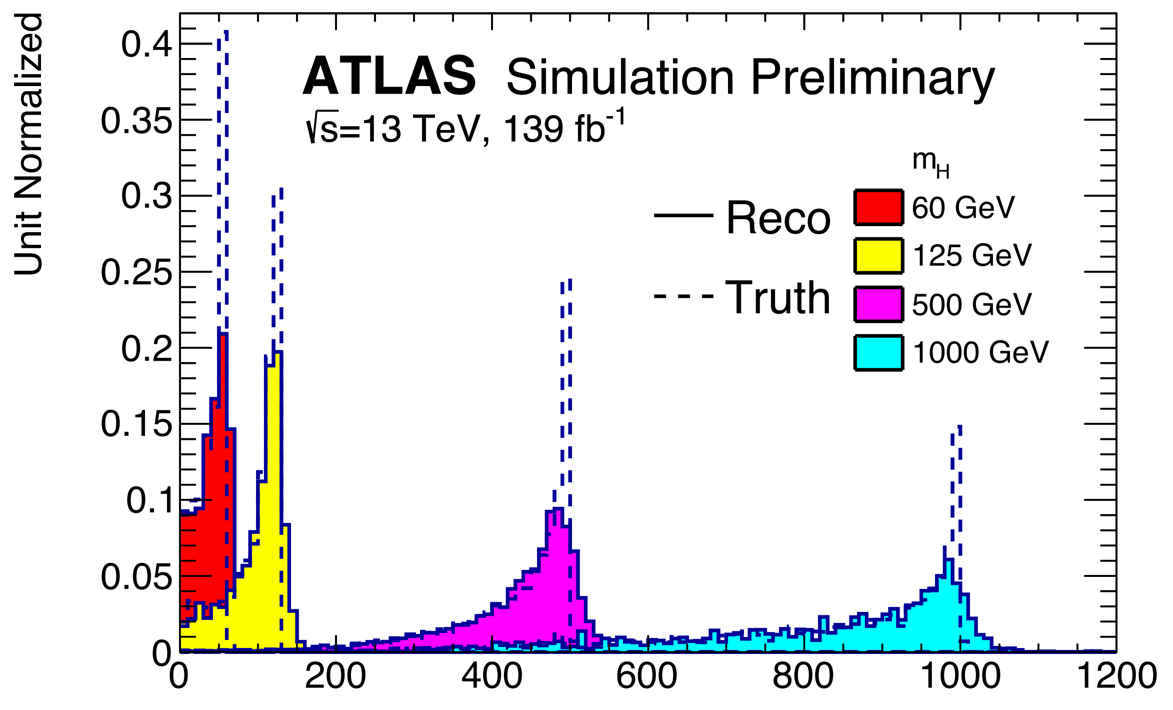

[ATLAS-CONF-2021-004]

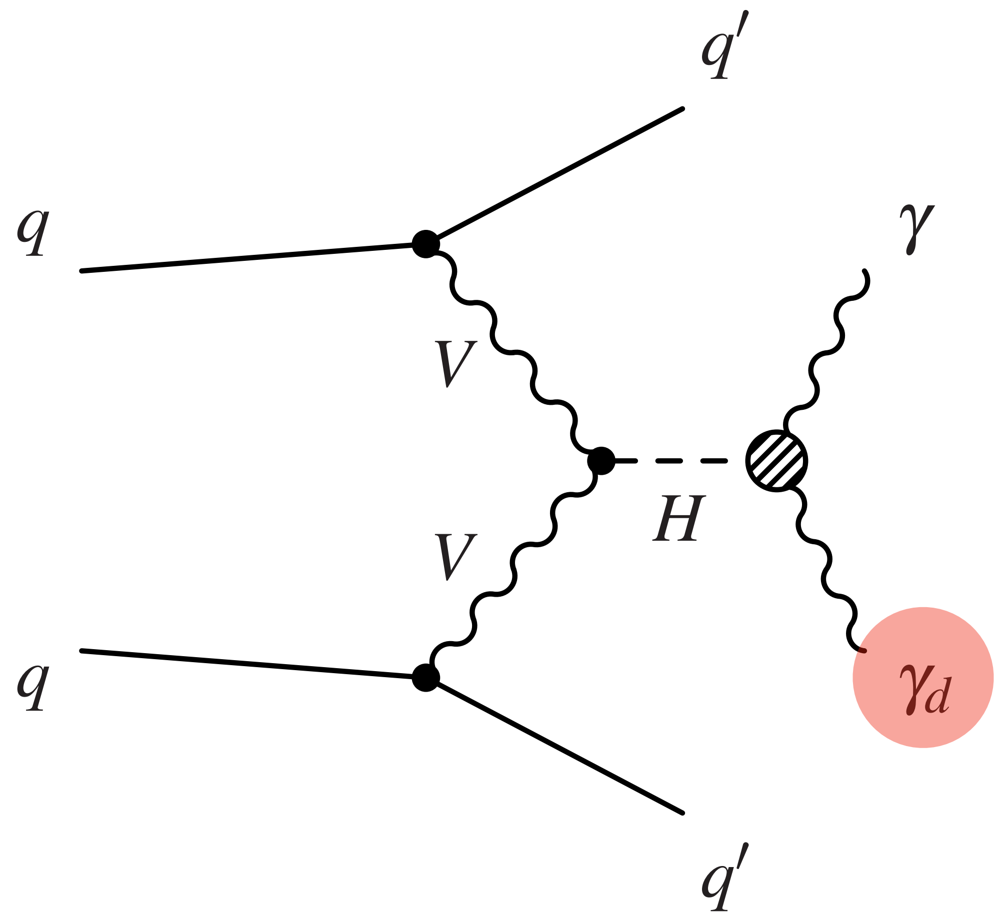

[ATLAS-CONF-2021-004]

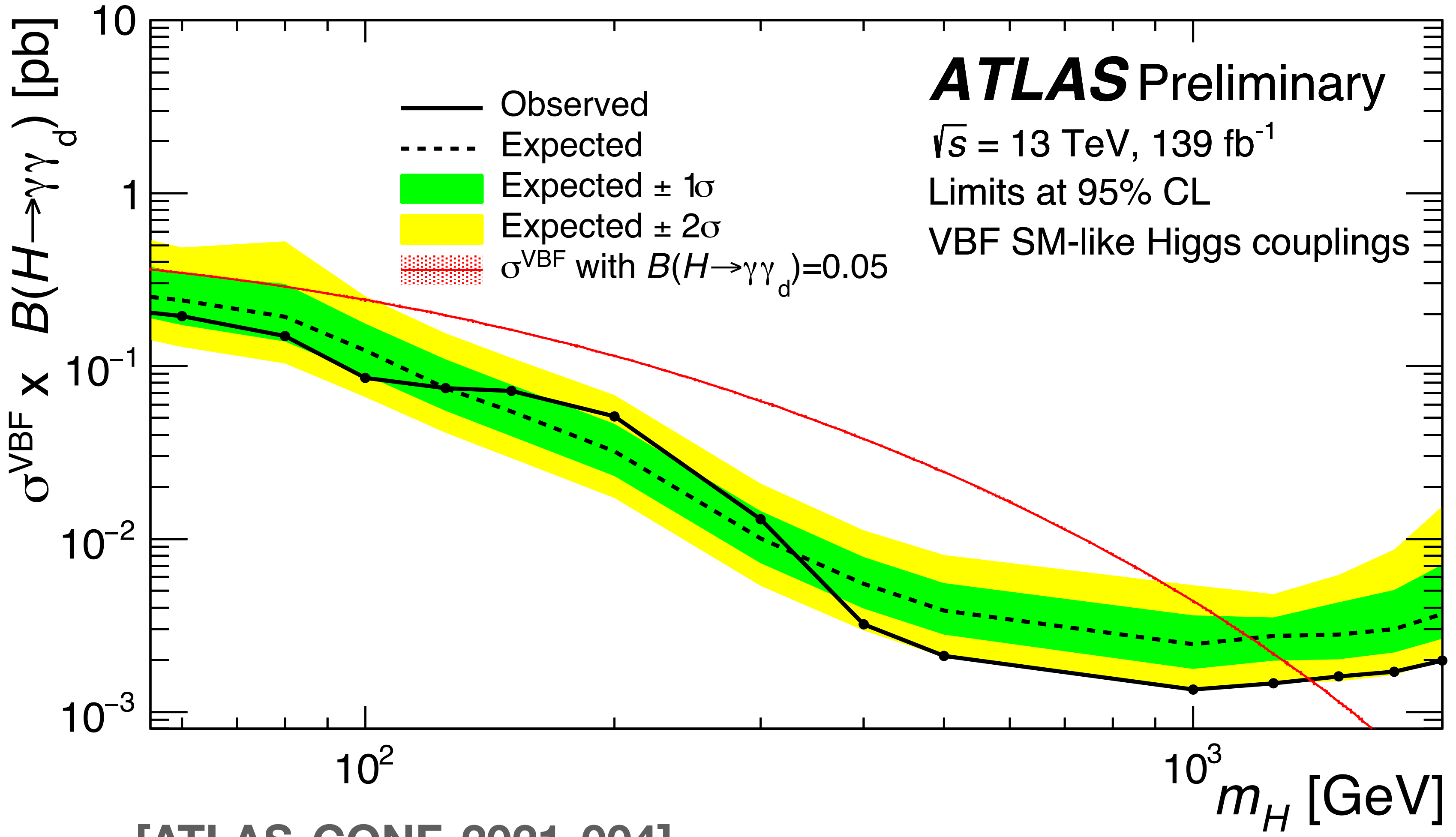

[ATLAS-CONF-2021-004]

excluded up to ~2 TeV

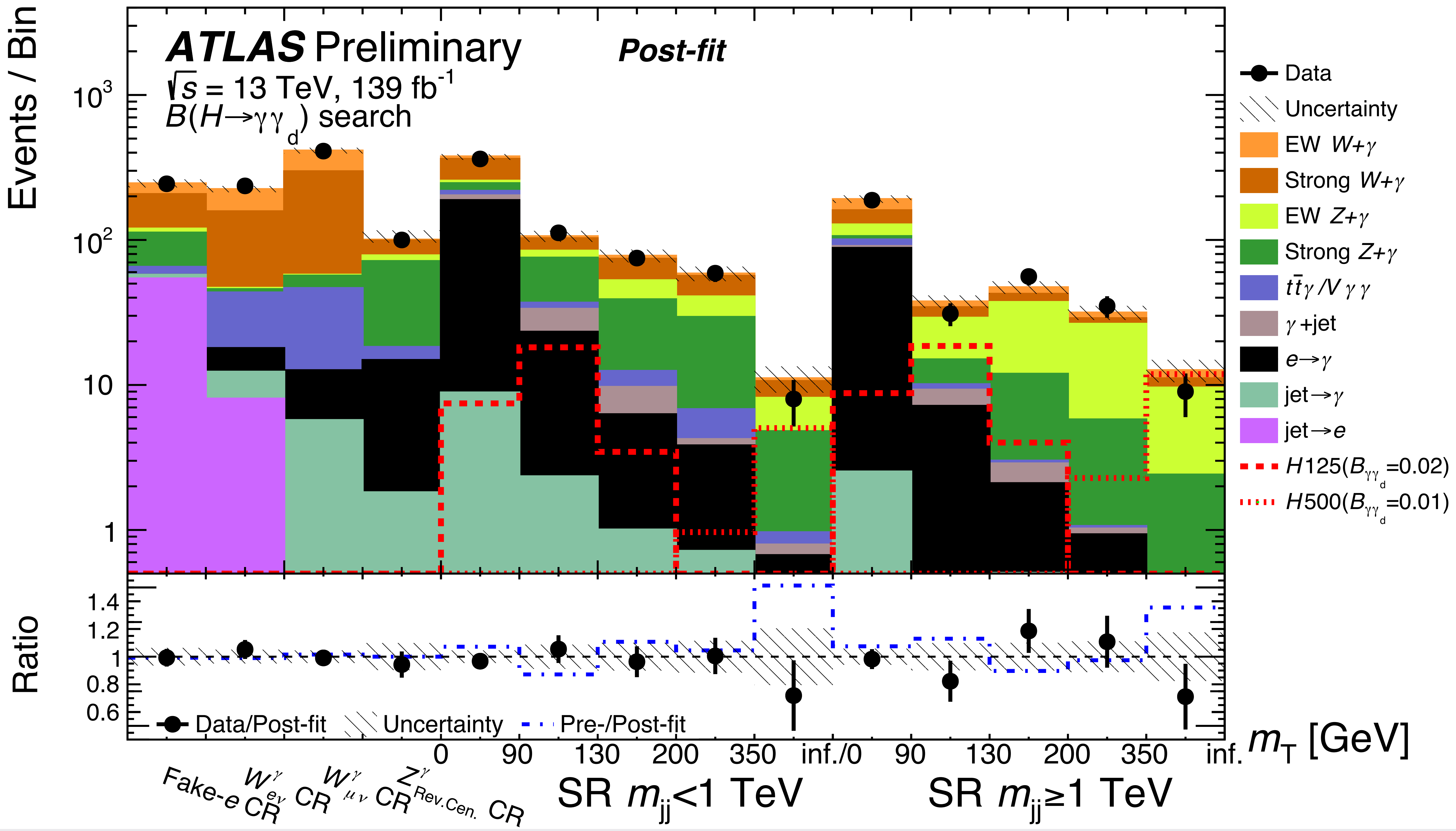

VBF H→inv

[ATLAS-CONF-2020-008]

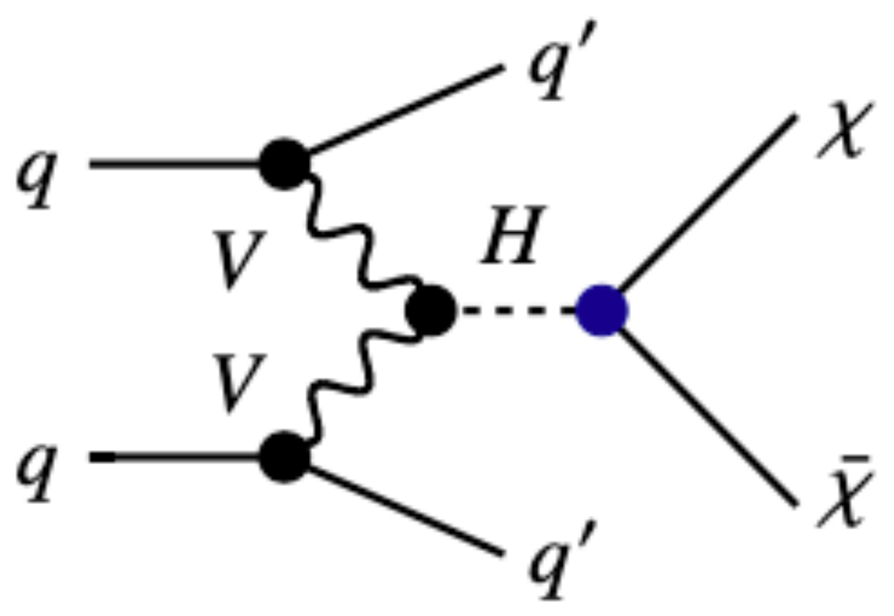

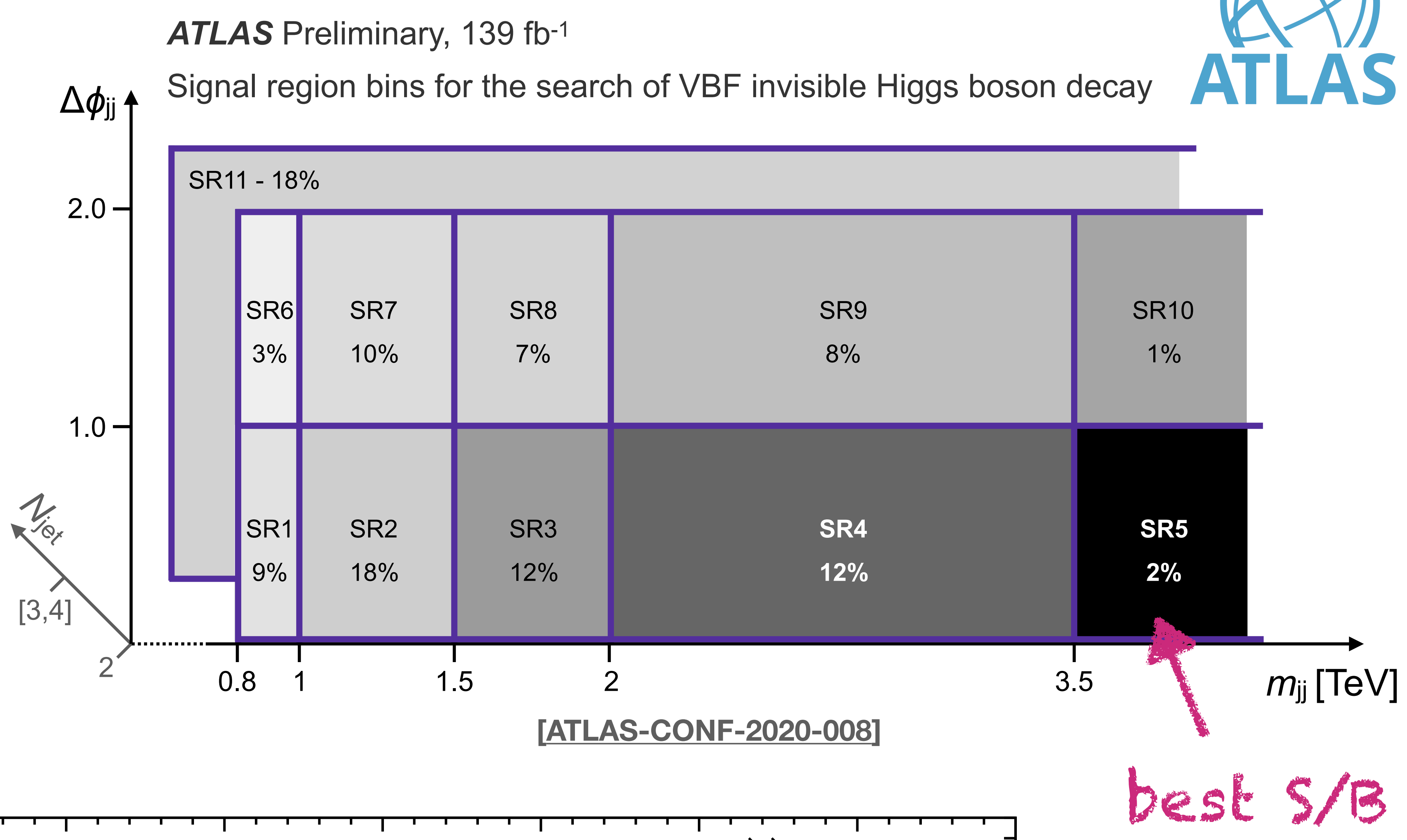

Two jets in the final state with distinctive features

- large invariant mass $m_{jj} > 0.8$ TeV
- large pseudo-rapidity separation $\Delta\eta_{jj} > 3.8$
- large missing transverse momentum $E_T^{miss} > 200$ GeV

Split into 11 signal region bins

Several CR to constrain the background contributions

- V+jets background ($Z_{\nu\nu}$, $W_{\ell\nu}$)

lepton lost in reconstruction

- Multijet background estimated from data

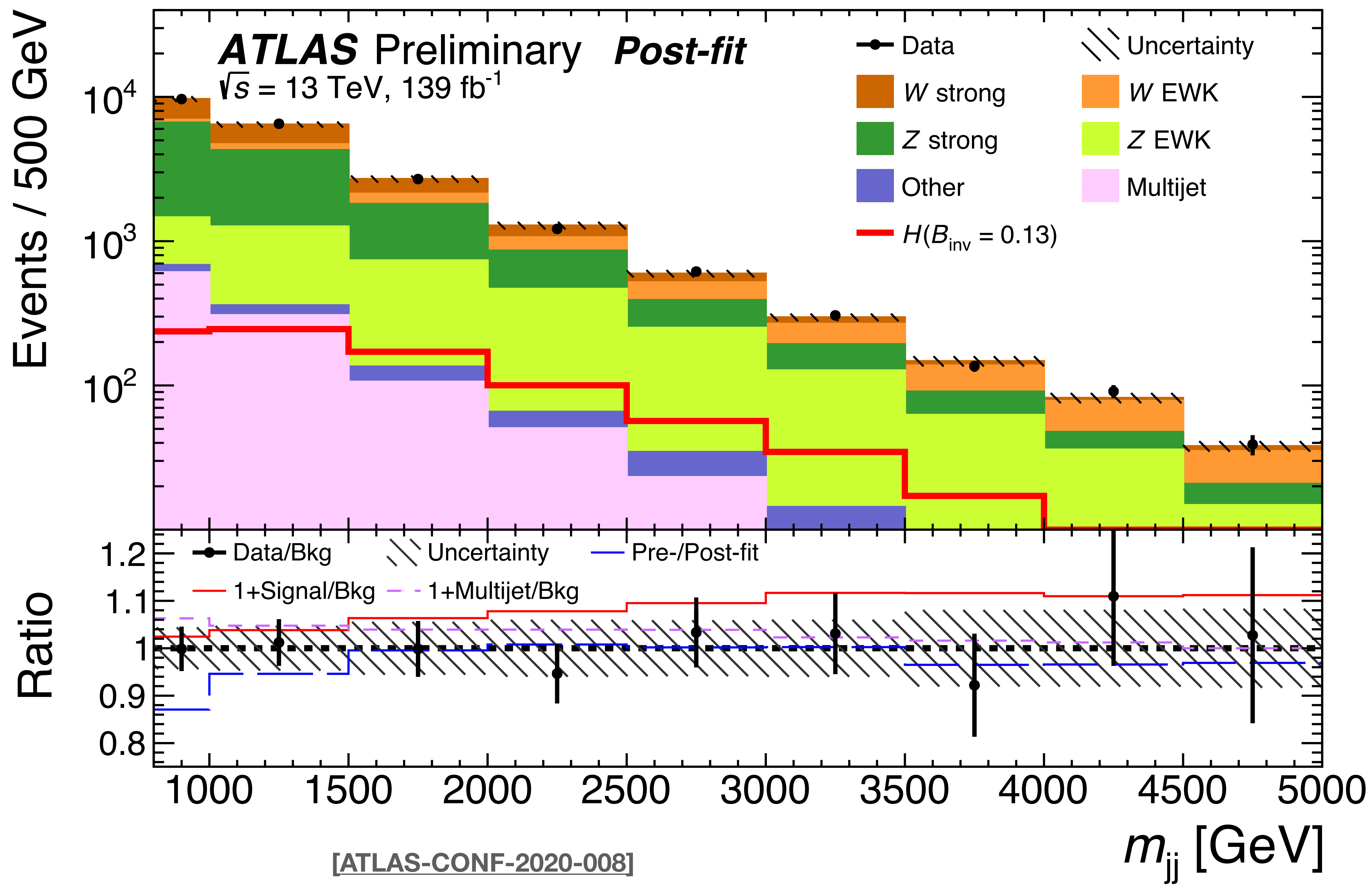

[ATLAS-CONF-2020-008]

VBF H→inv *results*

Full Run 2 result with 139 fb-1

Observed (expected) upper limit on the invisible Higgs boson branching ratio of

$BR_{H\to inv} < 0.13\ (0.13^{+0.05}_{-0.04})$

at 95% CL

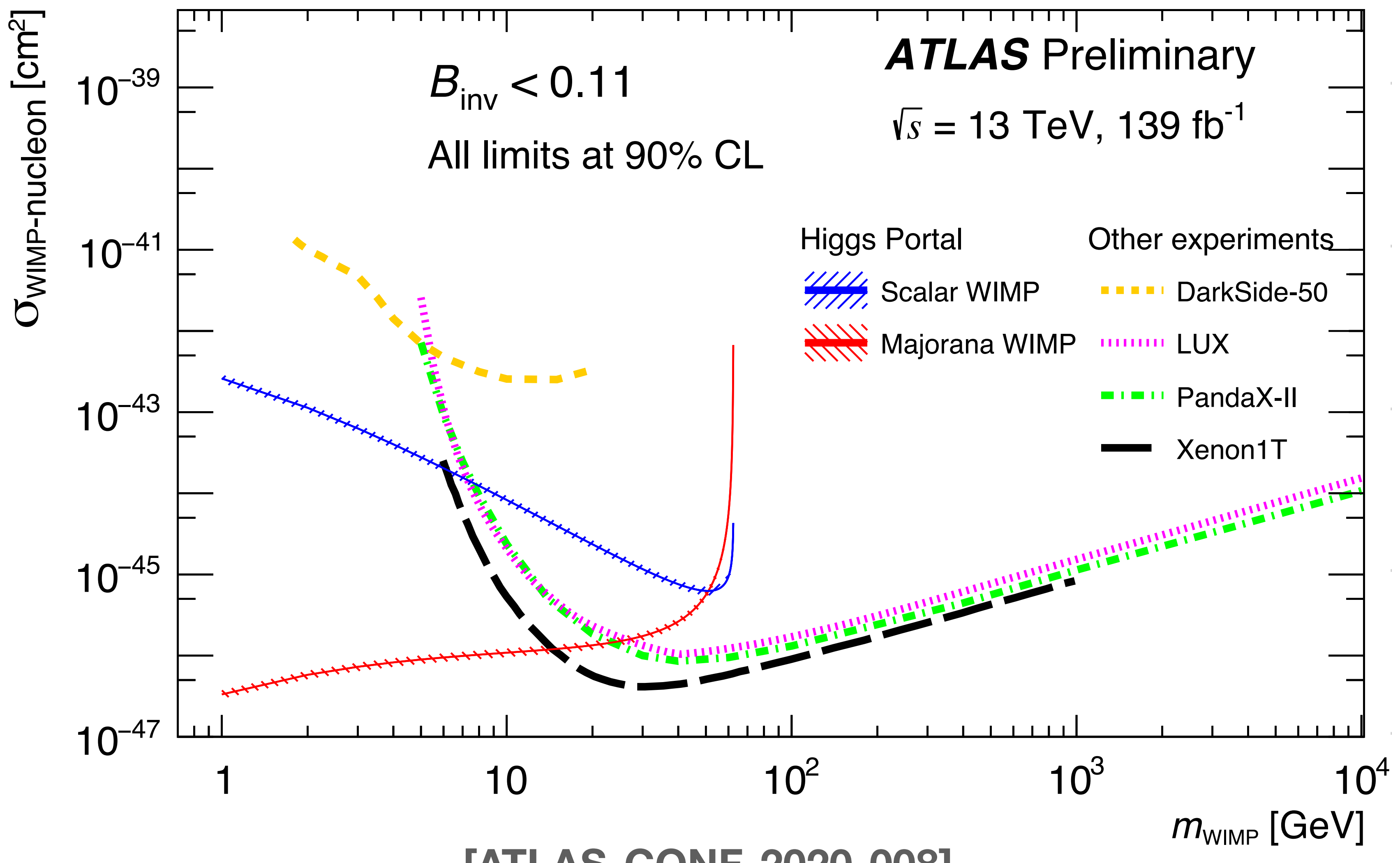

[ATLAS-CONF-2020-008]

Source	Δ [%]
Jet energy scale	1.8
Jet energy resolution	5.5
Lepton	4.6
Other	1.9
Multijet	7.0
V+jets theory	1.6
Signal theory	1.0
MC stats.	7.9
Data stats.	17.3

H→inv combination

[ATLAS-CONF-2020-052]

Full Run 2 combination

Includes as inputs:

1. search for invisible decays of the Higgs boson in the VBF topology [ATLAS-CONF-2020-008]
2. search for invisible decays of the Higgs boson in the *ttH* topology in 0l and 2l channels [Eur.Phys.J.C 80 (2020) 8, 737], [ATLAS-CONF-2020-046]
   ↞ *reinterpretation*
3. Run 1 combination [JHEP 11 (2015) 206] ↞ observed (expected) upper limit on BR_{inv} of 0.23 (0.24) ↞ *additionally includes a more general coupling fit*

1

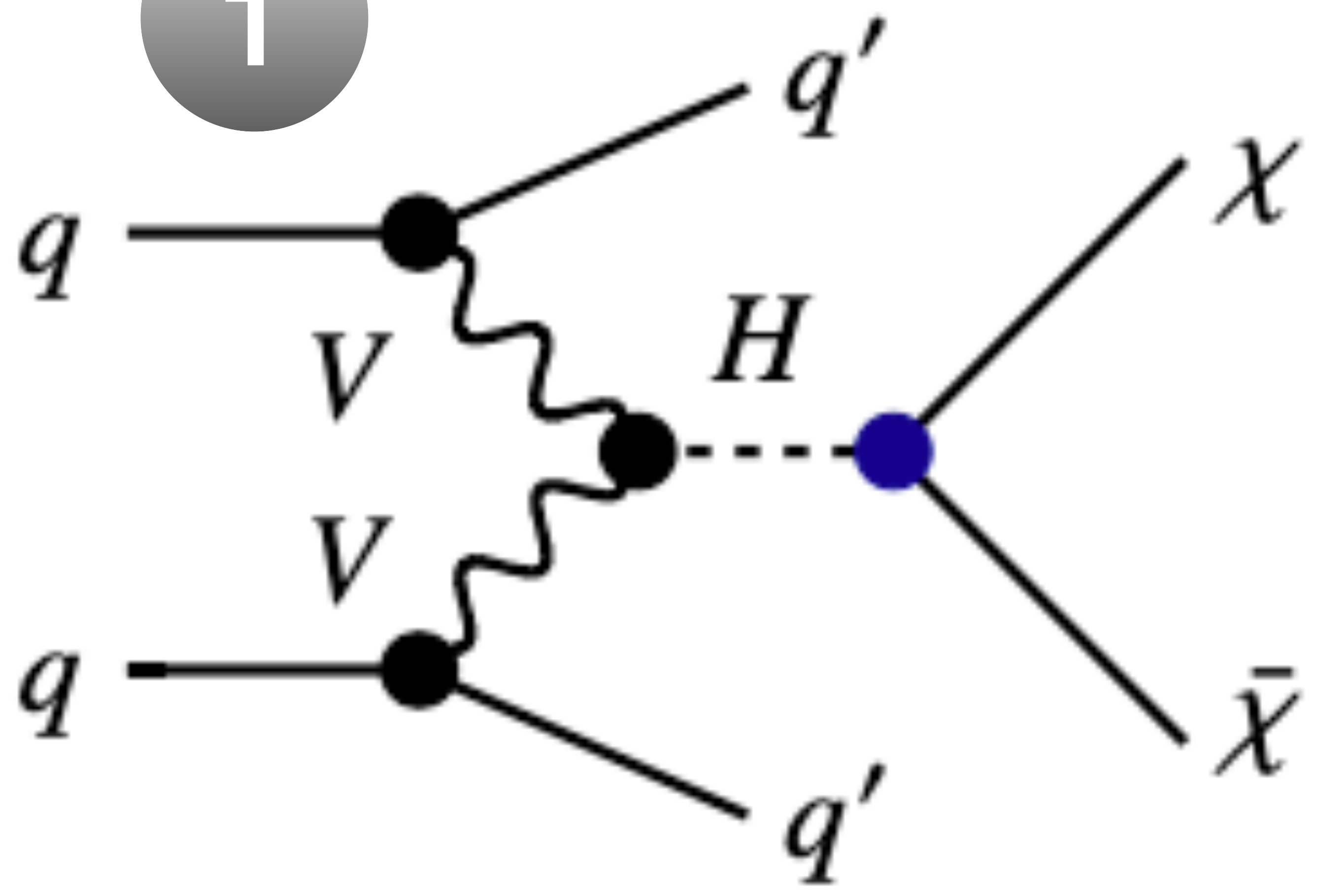

2

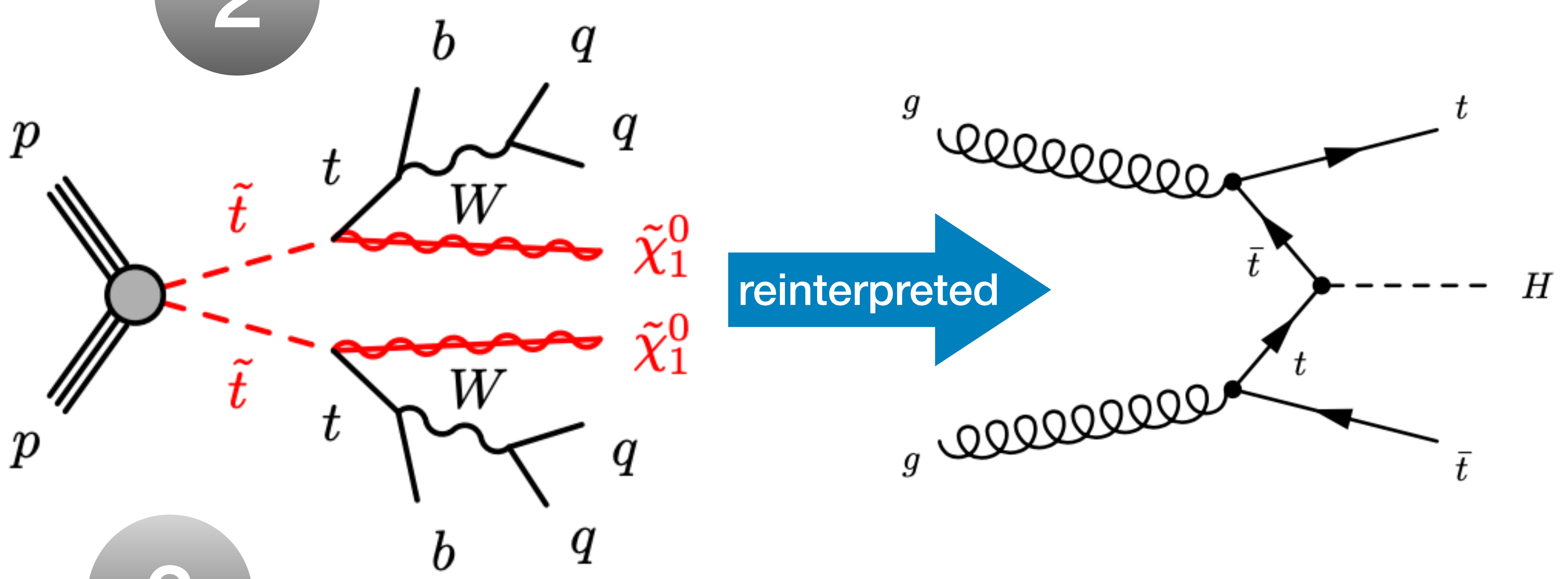

3

Channels	Upper limit on BR($h \to$ inv.) at the 95% CL					
	Obs.	−2 std. dev.	−1 std. dev.	Exp.	+1 std. dev.	+2 std. dev.
VBF h	0.28	0.17	0.23	0.31	0.44	0.60
$Z(\to \ell\ell)h$	0.75	0.33	0.45	0.62	0.86	1.19
$V(\to jj)h$	0.78	0.46	0.62	0.86	1.19	1.60
Combined Results	0.25	0.14	0.19	0.27	0.37	0.50

H→inv combination *results*

[ATLAS-CONF-2020-052]

Observed (expected) upper limit on the invisible Higgs boson branching ratio of

$BR_{H\rightarrow inv} < 0.11\ (0.11^{+0.04}_{-0.03})$

at 95% CL

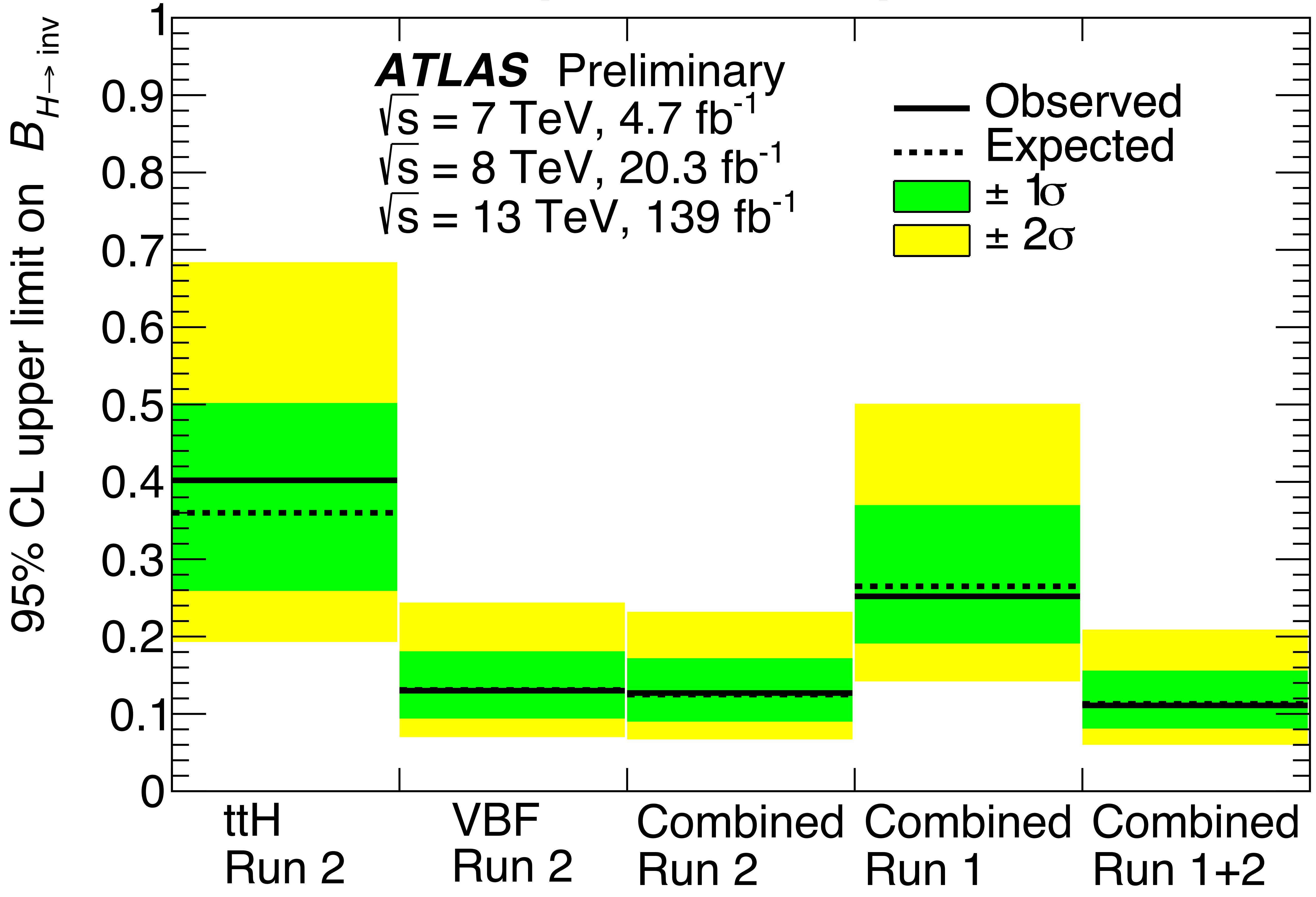

strongest individual constraint

Conclusion

Full Run 2 results of searches of DM produced *via* a Higgs boson or *in association with* a Higgs boson

- Results in the **Mono-Higgs** signature in the $b\bar{b}$ and $\gamma\gamma$ channel
- New **H→inv+photon** analysis presented that was performed for the first time
- The results on the **H→inv** branching ratio improved in the combination to an upper limit of $BR_{H\to inv} < 0.11$ $(0.11^{+0.04}_{-0.03})$
- More exciting results coming out (e.g. [ATLAS-CONF-2020-034]) that allow to further explore the parameter space (see also Guglielmo's talk on DM searches!)
- Maybe the Higgs boson can help understand some of the properties of the dark sector!

[ATLAS-CONF-2021-006]

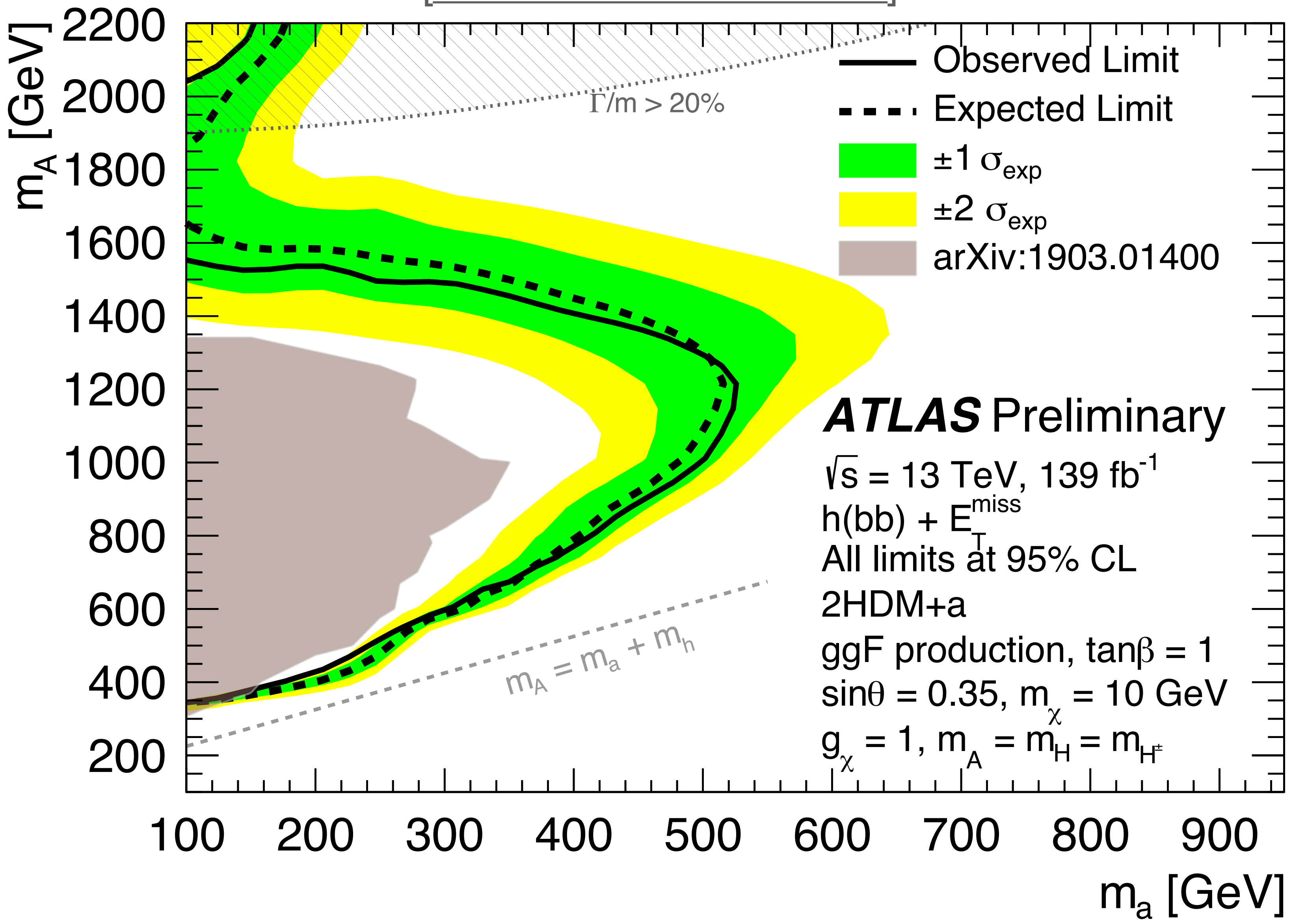

[ATLAS-CONF-2020-054]

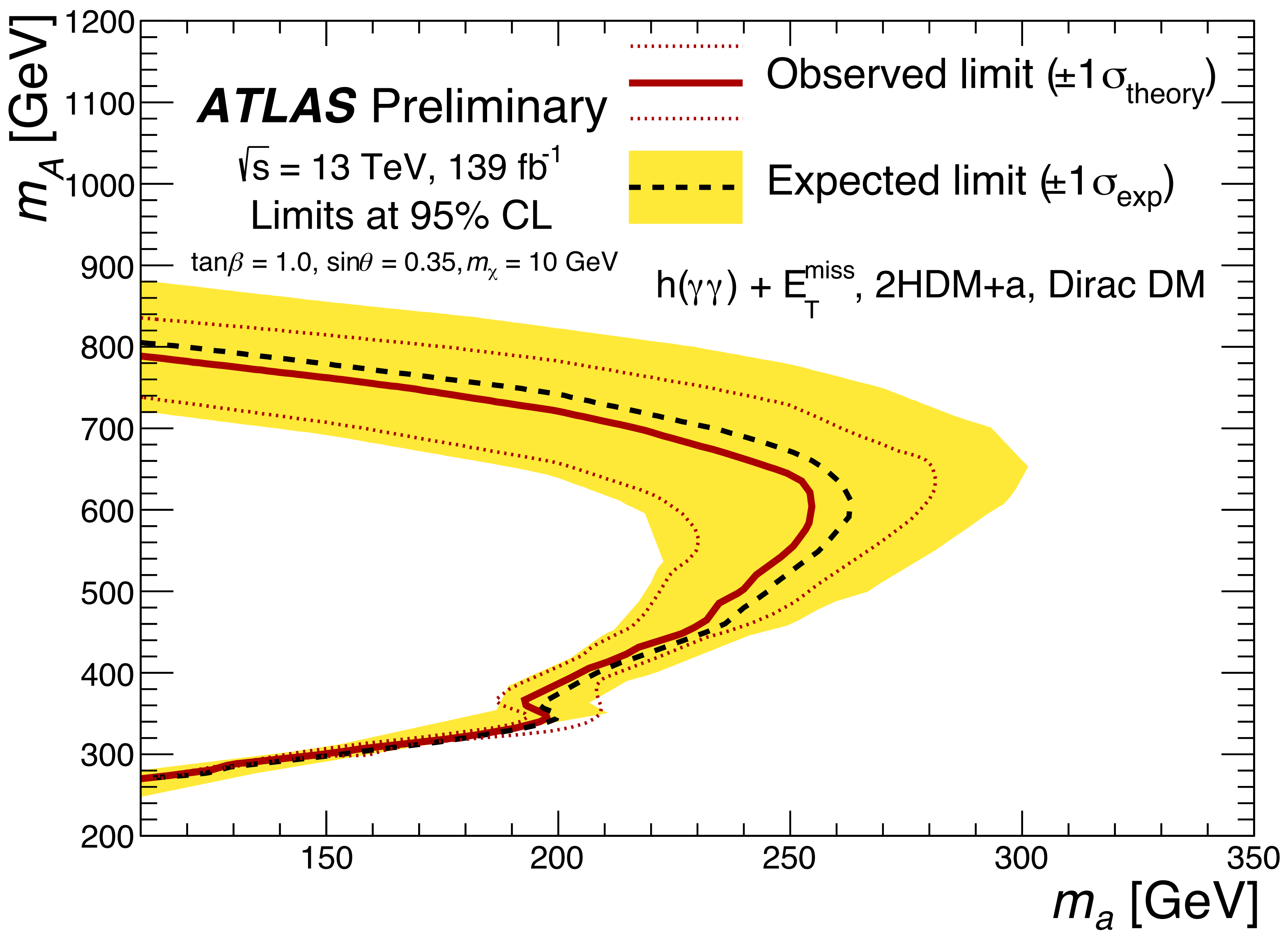

[ATLAS-CONF-2020-052]

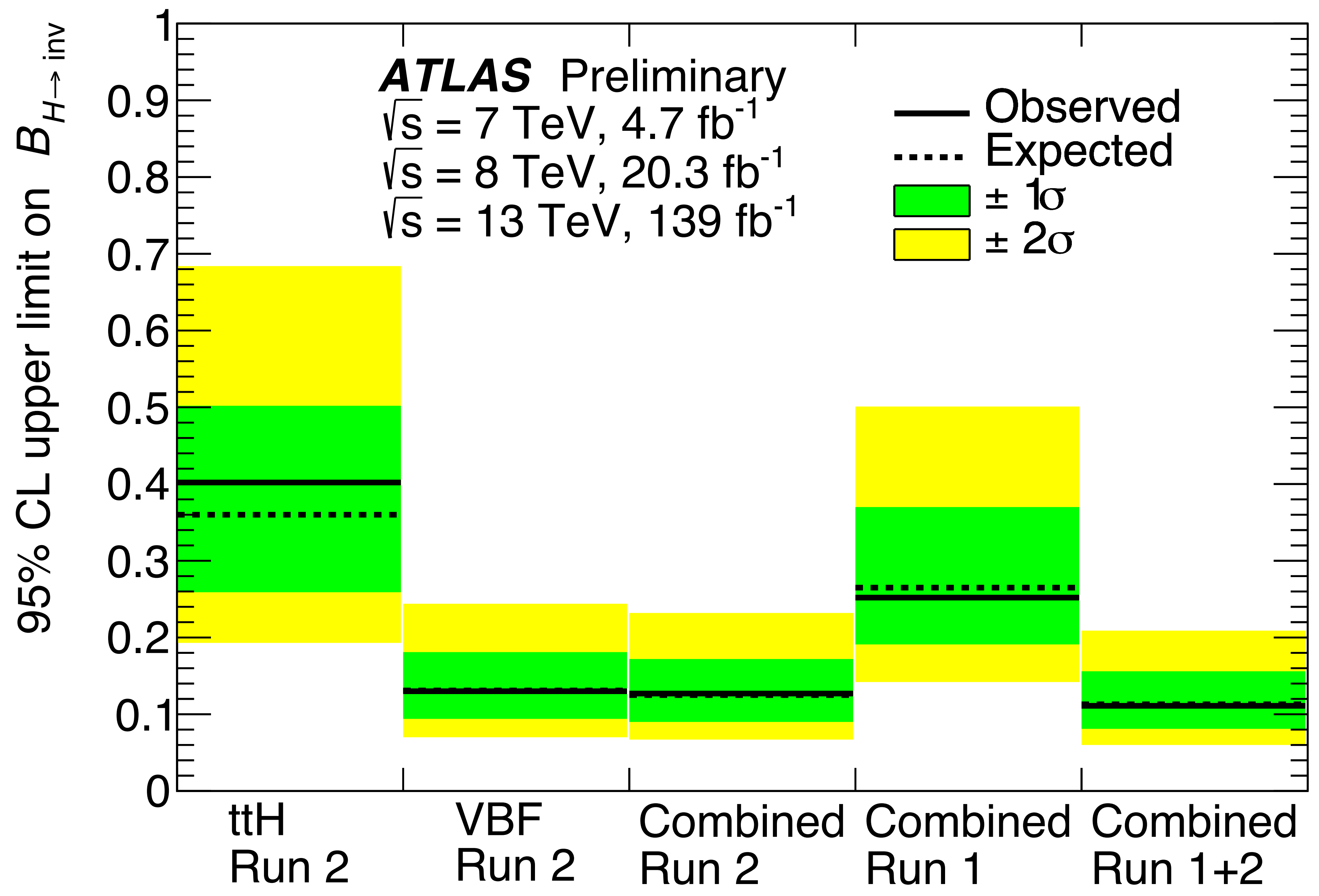

BACKUP

Mono-H($b\bar{b}$)

Resolved	Merged
Primary $E_{\mathrm{T}}^{\mathrm{miss}}$ trigger	
Data quality selections	
$E_{\mathrm{T}}^{\mathrm{miss}} > 150$ GeV	
Lepton veto & extended τ-lepton veto	
$\Delta\phi(\mathrm{jet}_{1,2,3}, E_{\mathrm{T}}^{\mathrm{miss}}) > 20°$	
$E_{\mathrm{T}}^{\mathrm{miss}} < 500$ GeV	$E_{\mathrm{T}}^{\mathrm{miss}} > 500$ GeV
At least 2 small-R jets	At least 1 large-R jet
At least 2 b-tagged small-R jets	At least 2 b-tagged associated variable-R track jets
$p_{\mathrm{T}h} > 100$ GeV if $E_{\mathrm{T}}^{\mathrm{miss}} < 350$ GeV $p_{\mathrm{T}h} > 300$ GeV if $E_{\mathrm{T}}^{\mathrm{miss}} > 350$ GeV	—
$m_{\mathrm{T}}^{b,\mathrm{min}} > 170$ GeV	—
$m_{\mathrm{T}}^{b,\mathrm{max}} > 200$ GeV	—
$\mathcal{S} > 12$	—
$N_{\text{small-}R\text{ jets}} \leq 4$ if 2 b-tag $N_{\text{small-}R\text{ jets}} \leq 5$ if ≥ 3 b-tag	—
50 GeV $< m_h <$ 280 GeV	50 GeV $< m_h <$ 270 GeV

Source of uncertainty	Fractional squared uncertainty on μ		
	Z'-2HDM signals, (m'_Z, m_A) [GeV]		
	(800, 500)	(1400, 1000)	(2800, 300)
Z+HF normalisation	0.11	0.03	<0.01
W+HF normalisation	0.02	0.01	<0.01
$t\bar{t}$ normalisation	0.16	0.04	<0.01
Z modelling uncertainties	0.02	0.07	<0.01
W modelling uncertainties	<0.01	0.01	<0.01
$t\bar{t}$ modelling uncertainties	0.13	0.05	<0.01
Single t modelling uncertainties	0.18	0.02	<0.01
Other modelling uncertainties	0.05	0.01	<0.01
Jets	0.20	0.06	0.01
b-tagging	0.01	0.01	0.04
$E_{\mathrm{T}}^{\mathrm{miss}}$ soft term and pile-up	<0.01	<0.01	<0.01
Other experimental systematic uncertainties	0.01	<0.01	<0.01
Signal systematic uncertainties	<0.01	<0.01	<0.01
MC sample statistics	0.08	0.07	0.11
Statistical uncertainty	0.27	0.61	0.79
Total systematic uncertainties	0.73	0.39	0.21

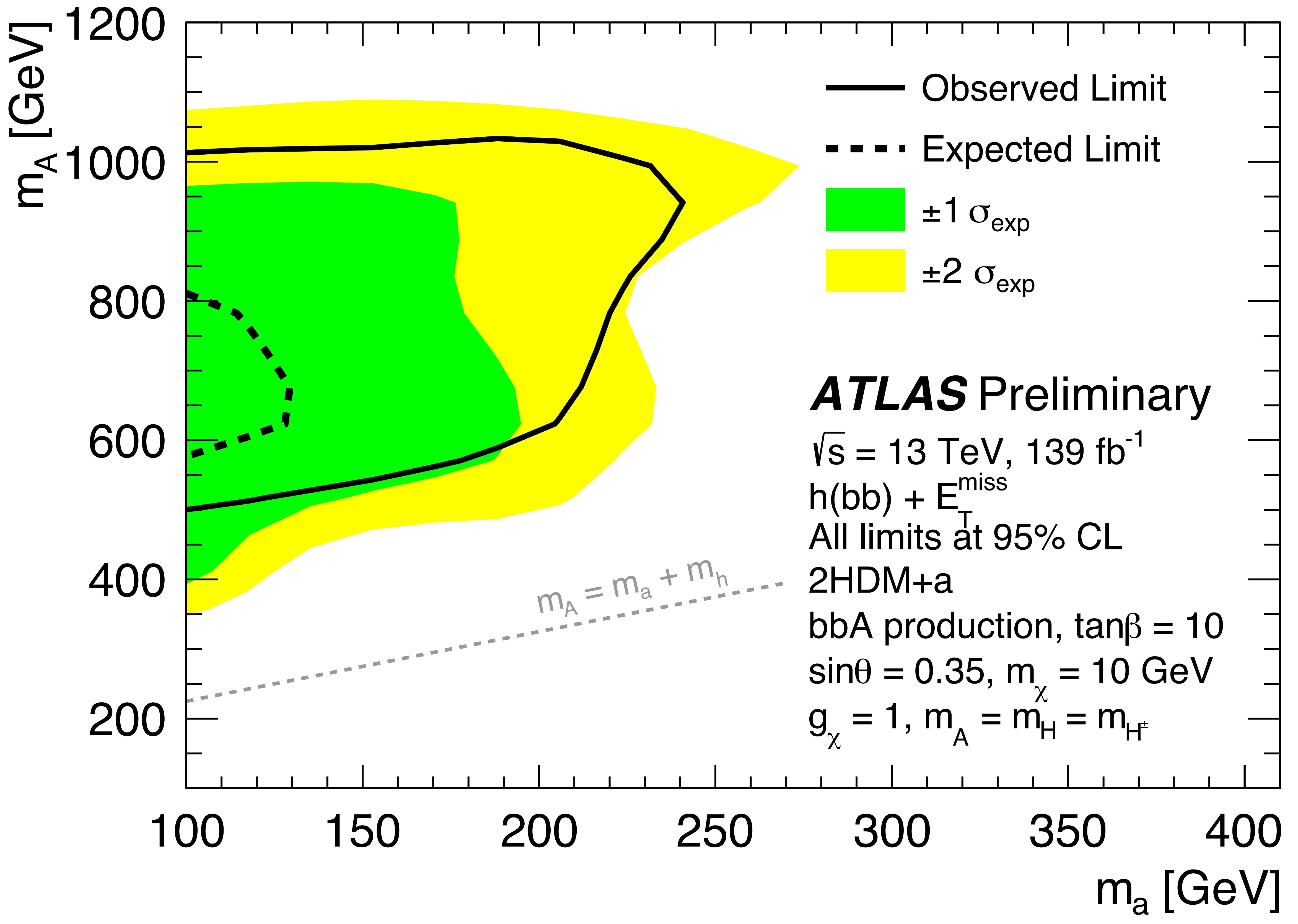

Mono-H($\gamma\gamma$)

Uncertainties

Source	Signals [%]	Backgrounds [%] SM Higgs boson	Backgrounds [%] Non-resonant background
Experimental			
Luminosity	1.7	1.7	-
Trigger efficiency	1.0	1.0	-
Vertex selection (inclusive cat.)	0.01	0.01	-
Photon energy scale	1.0	1.2	-
Photon energy resolution	0.3	0.4	-
Photon identification efficiency	1.3	1.3	-
Photon isolation efficiency	1.3	1.4	-
ATLFASTII simulation	2.0	–	-
E_T^{miss} reconstruction and jet uncertainty	2.8	1.7	-
Pile-up reweighting	2.3	2.0	-
Signal efficiency interpolation	< 13	–	-
Non-resonant background modelling	–	–	6.8
Theoretical			
Factorization and renormalization scale in migration	1.3	3.5	-
PDF+α_S in migration	1.2	1.0	-
Factorization and renormalization scale in cross section	–	2.8	-
PDF+α_S in cross section	–	2.8	-
Multi-parton interactions, ISR/FSR, hadronization	3.0	3.0	-
$B(H \to \gamma\gamma)$	1.7	1.7	-

Post-fit event yields:

Category	High E_T^{miss} BDT tight	High E_T^{miss} BDT loose	Low E_T^{miss} BDT tight	Low E_T^{miss} BDT loose
Data	12	29	11	143
Backgrounds				
SM Higgs boson	3.74 ± 0.25	3.40 ± 0.28	3.12 ± 0.23	9.9 ± 1.5
Non-resonant	7.8 ± 1.3	25.3 ± 2.3	9.8 ± 1.5	130 ± 5
Total	11.6 ± 1.3	28.7 ± 2.3	12.9 ± 1.5	140 ± 5
Z'_B model, $m_{Z'_B}$ = 1000 GeV, m_χ = 50 GeV				
Signal yields	0.7 ± 3.1	0.1 ± 0.6	0.1 ± 0.6	0.1 ± 0.6
Z'-2HDM model, m_A = 800 GeV and m_χ = 500 GeV				
Signal yields	0.6 ± 3.1	0.1 ± 0.4	0.05 ± 0.26	0.03 ± 0.17
2HDM+a model, m_A = 600 GeV, m_a = 200 GeV, $\tan\beta$ = 1.0, $\sin\theta$ = 0.35				
Signal yields	0.6 ± 3.1	0.2 ± 1.2	0.1 ± 0.5	0.1 ± 0.7

Category	Category name	Selection
1	high E_T^{miss}, BDT tight	$E_T^{miss} > 150$ GeV, $0.950 <$ BDT score < 1
2	high E_T^{miss}, BDT loose	$E_T^{miss} > 150$ GeV, $0.694 <$ BDT score < 0.950
3	low E_T^{miss}, BDT tight	$E_T^{miss} < 150$ GeV, $0.864 <$ BDT score < 1
4	low E_T^{miss}, BDT loose	$E_T^{miss} < 150$ GeV, $0.386 <$ BDT score < 0.864

2HDM+a

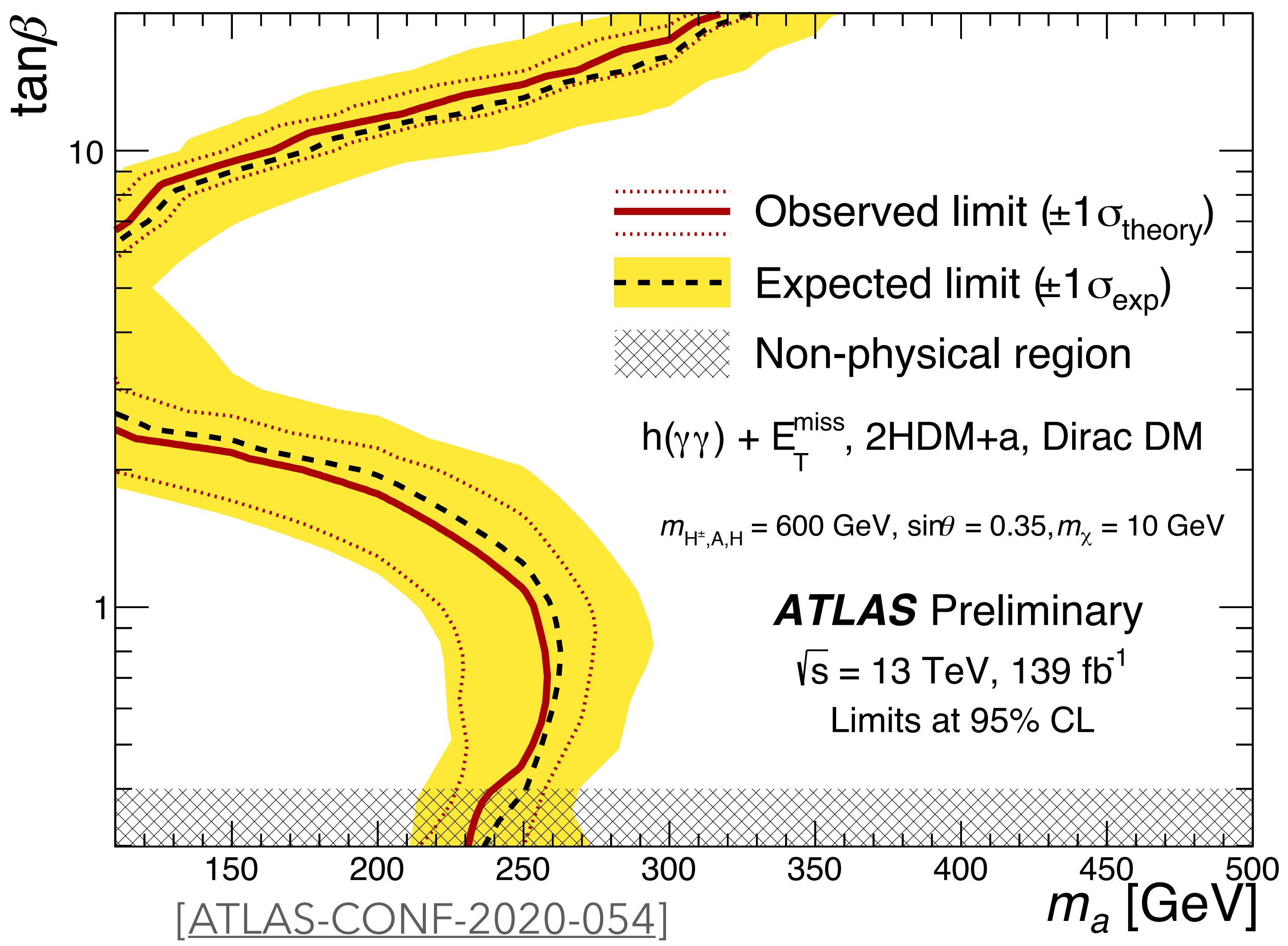

[ATLAS-CONF-2020-054]

Z'B

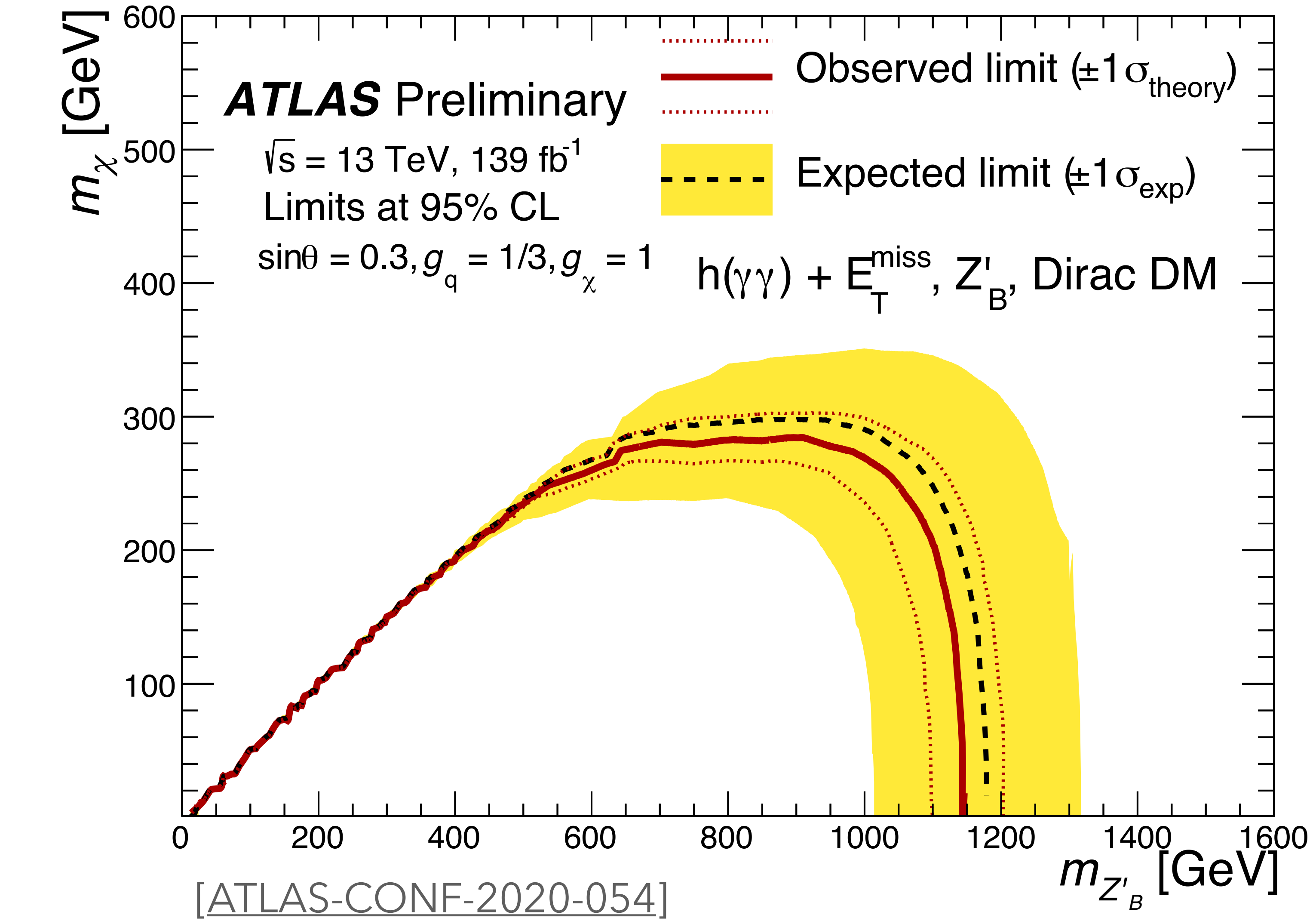

[ATLAS-CONF-2020-054]

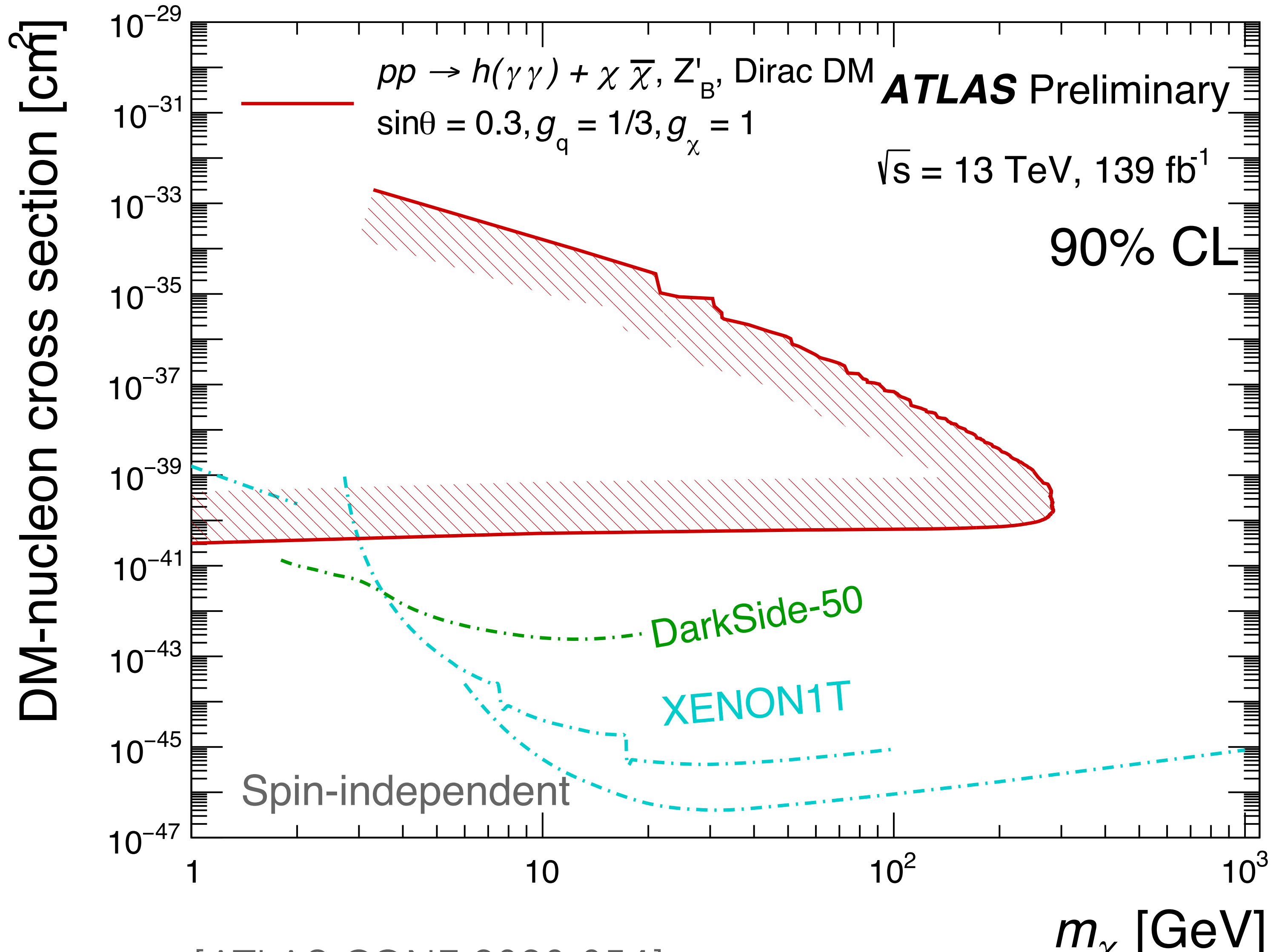

[ATLAS-CONF-2020-054]

VBF H→inv

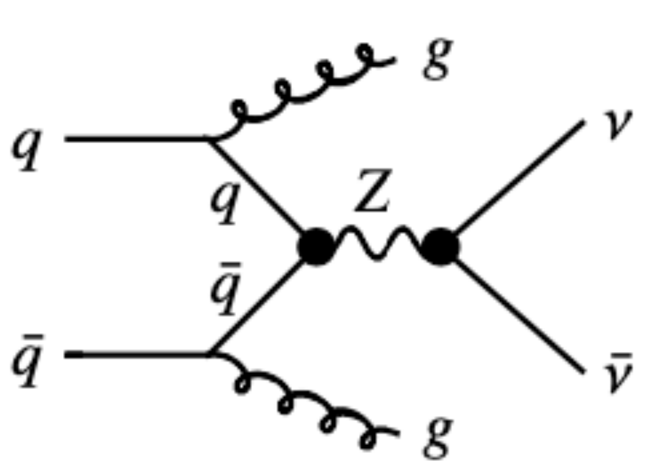

(b) Example diagram for the strong Z+jets back process

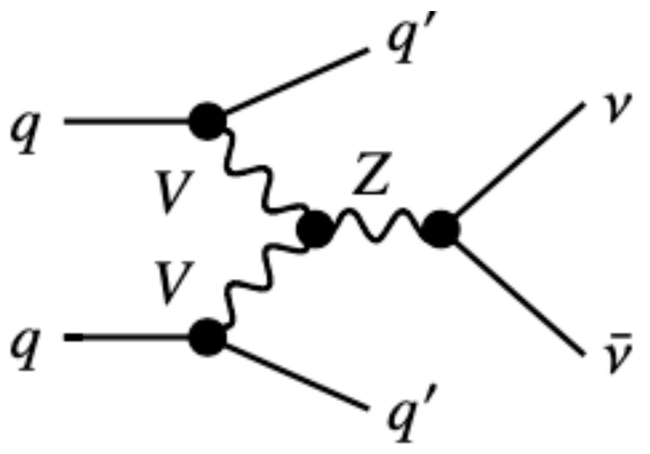

(c) Example diagram for the electroweak VBF Z+jets background process

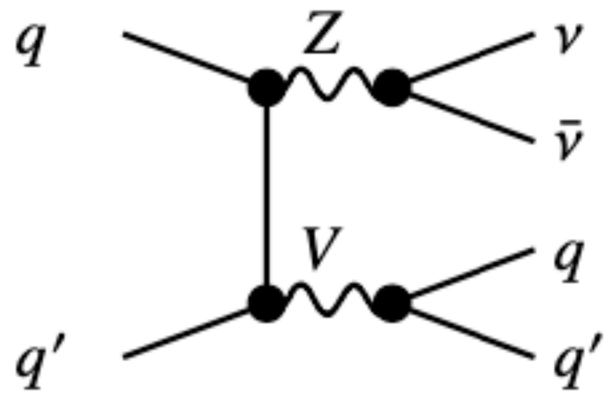

(d) Example diagram for the electroweak diboson process

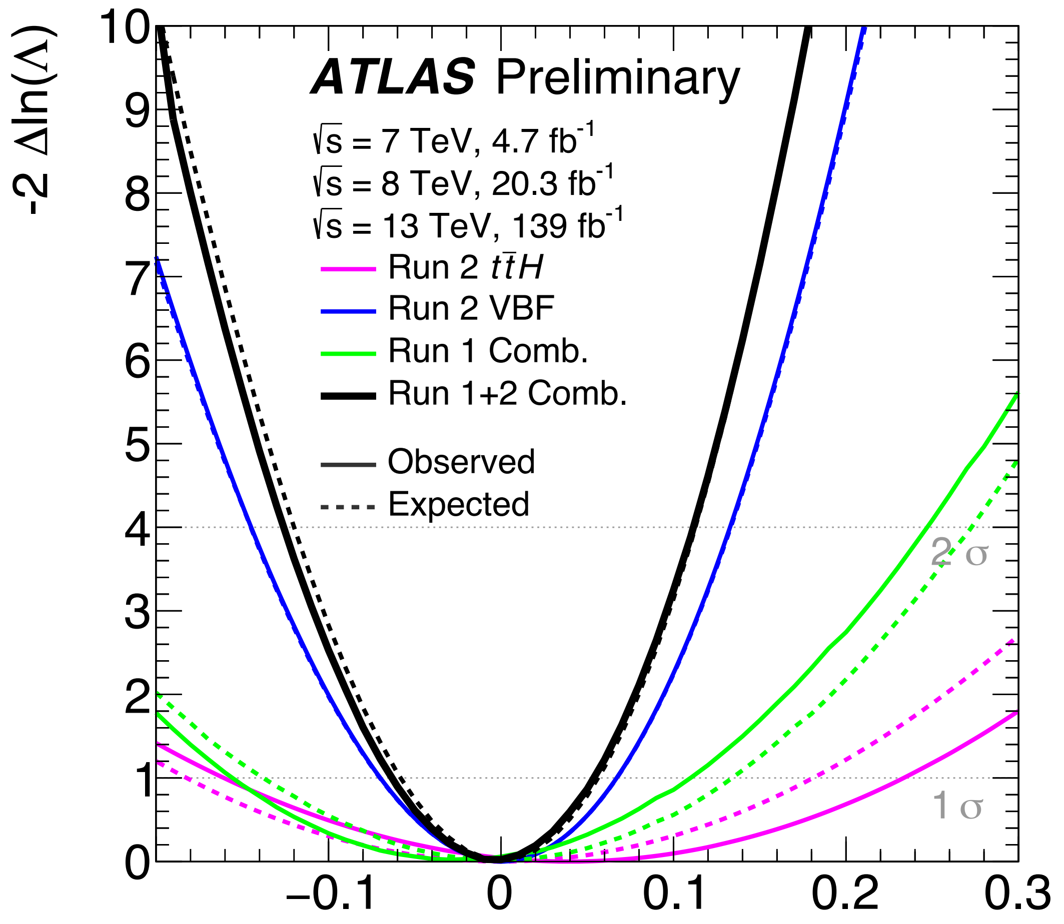

[ATLAS-CONF-2020-052]

$B_{H\to \text{inv}}$

Analysis	$\sqrt{s}$ [TeV]	Int. luminosity [fb^{-1}]	Best fit $\mathcal{B}_{H\to\text{inv}}$	Observed upper limit	Expected upper limit	Reference
Run 2 VBF	13	139	$0.00^{+0.07}_{-0.07}$	0.13	$0.13^{+0.05}_{-0.04}$	[42]
Run 2 $t\bar{t}H$	13	139	$0.04^{+0.20}_{-0.20}$	0.40	$0.36^{+0.15}_{-0.10}$	This document
Run 2 Comb.	13	139	$0.00^{+0.06}_{-0.07}$	0.13	$0.12^{+0.05}_{-0.04}$	This document
Run 1 Comb.	7, 8	4.7, 20.3	$-0.02^{+0.14}_{-0.13}$	0.25	$0.27^{+0.10}_{-0.08}$	[36]
Run 1+2 Comb.	7, 8, 13	4.7, 20.3, 139	$0.00^{+0.06}_{-0.06}$	0.11	$0.11^{+0.04}_{-0.03}$	This document

Source	Δ [%]
Jet energy scale	1.8
Jet energy resolution	5.5
Lepton	4.6
Other	1.9
Multijet	7.0
V+jets theory	1.6
Signal theory	1.0
MC stats.	7.9
Data stats.	17.3

Process	SR	$Z_{\ell\ell}$	$W_{e\nu}$	$W_{\mu\nu}$	$W_{\ell\nu}$	Fake-e CR
Z strong	6 810 ± 430	1 394 ± 81	48 ± 11	193 ± 21	241 ± 23	153 ± 18
Z EWK	2 660 ± 320	634 ± 75	12 ± 1	41 ± 2	53 ± 2	26 ± 2
W strong	3 750 ± 270	-	3 530 ± 230	6 730 ± 390	10 260 ± 610	1 760 ± 140
W EWK	1 380 ± 130	-	2 140 ± 210	3 770 ± 370	5 910 ± 570	1 120 ± 120
Fake-e	-	-	239 ± 62	-	239 ± 62	1 190 ± 180
Multijet	740 ± 280	-	-	-	-	-
Other	155 ± 27	37 ± 27	322 ± 50	395 ± 60	720 ± 110	57 ± 7
Tot. bg.	15 490 ± 130	2 065 ± 44	6 288 ± 75	11 130 ± 110	17 420 ± 150	4 300 ± 66
H (VBF)	647 ± 52	Predicted signal for $\mathcal{B}_{\text{inv}} = 13\%$ (observed limit)				
H (ggF)	90 ± 43					
H (VH)	0.81 ± 0.14					
Data	15 511	2 050	6 323	11 095	17 418	4 293

VBF H→inv

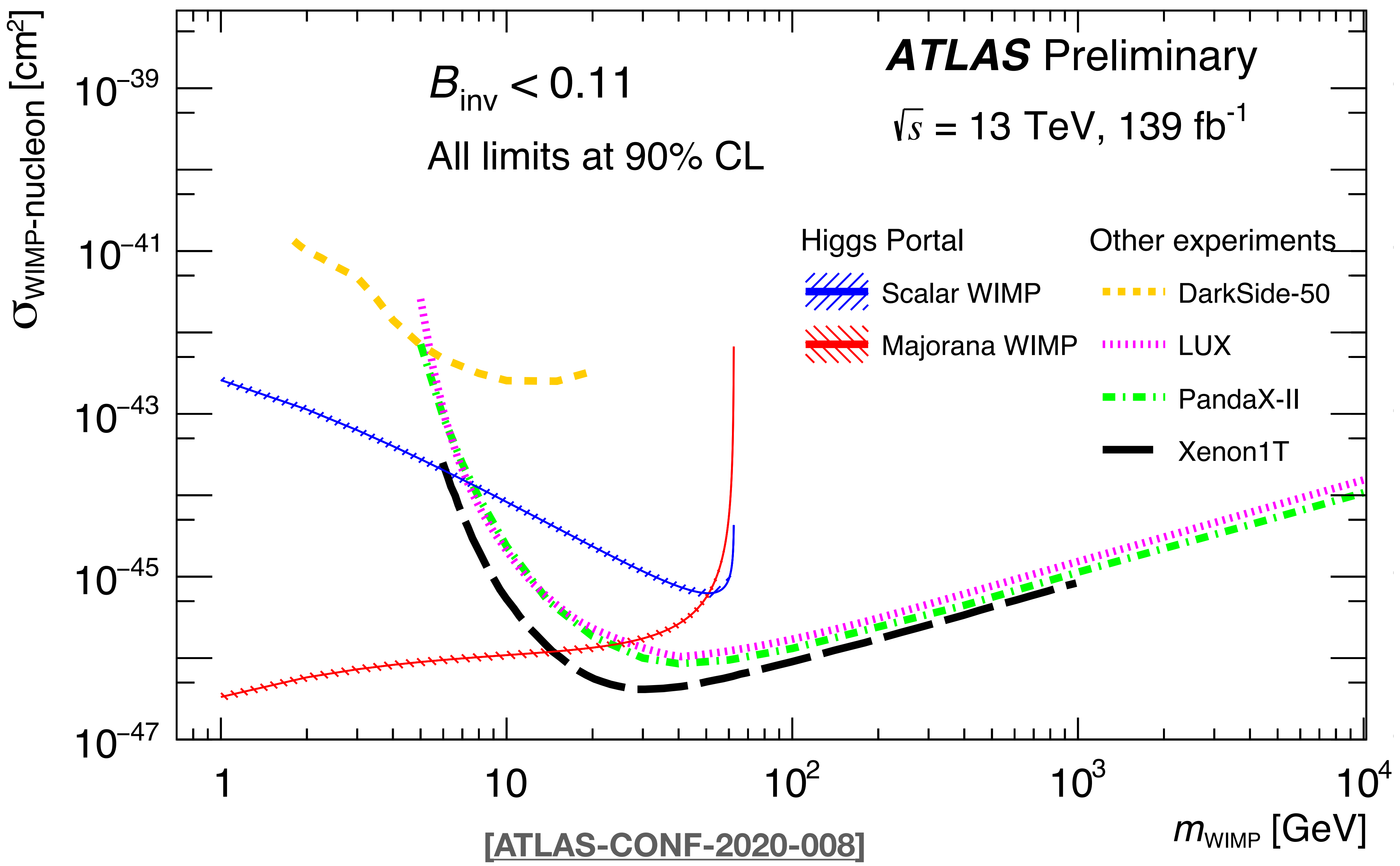

[ATLAS-CONF-2020-008]

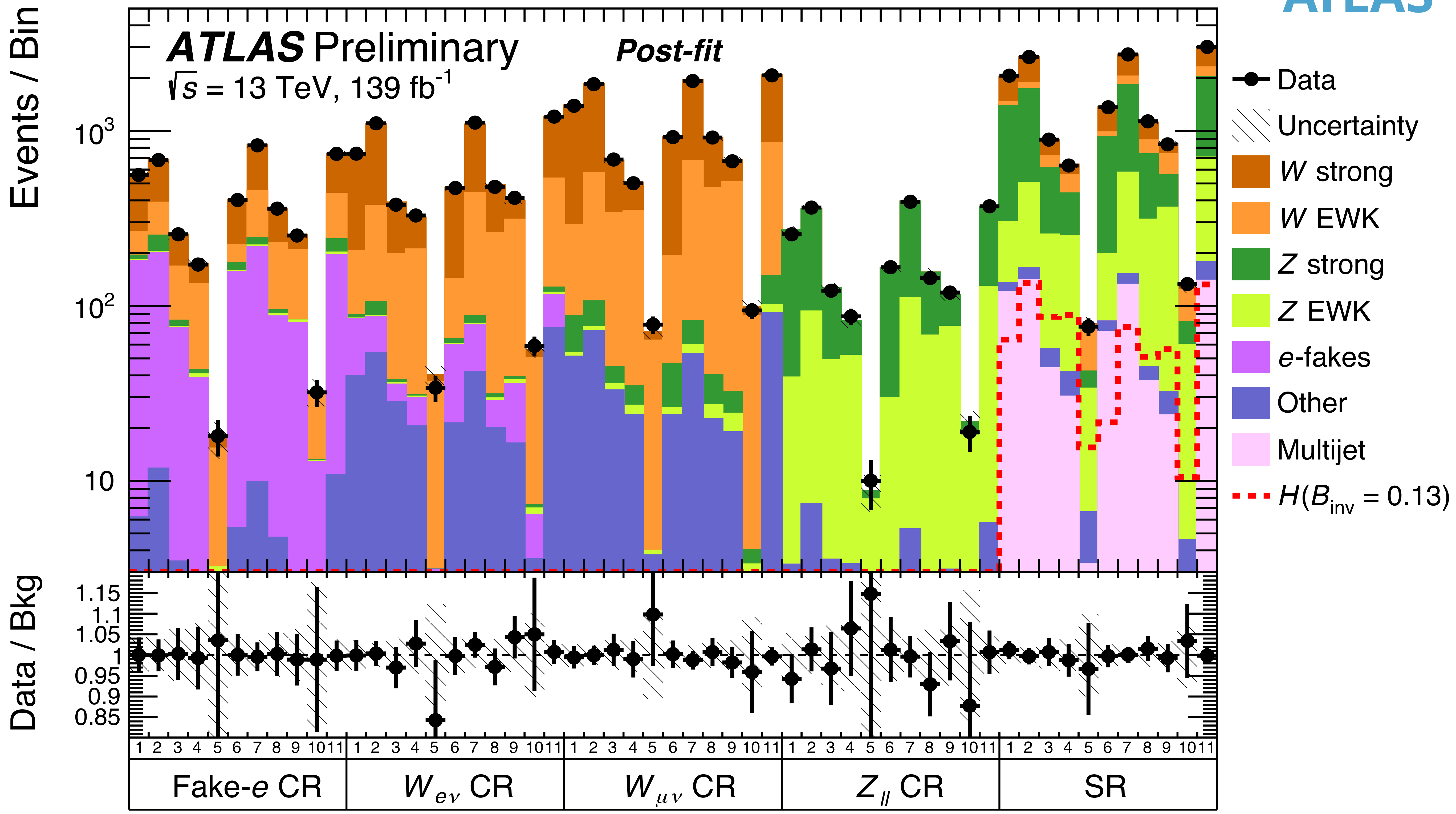

Table 11: Parameters in the Higgs-portal dark-matter model.

Vacuum expectation value	$v/\sqrt{2}$	174 GeV
Higgs boson mass	m_H	125 GeV
Higgs boson width	Γ_H	4.07 MeV
Nucleon mass	m_N	939 MeV
Higgs–nucleon coupling form factor	f_N	$0.33^{+0.30}_{-0.07}$

$$\sigma^{\mathrm{SI}}_{SN} = \frac{\lambda^2_{HSS}}{16\pi m^4_H}\frac{m^4_N f^2_N}{(m_S + m_N)^2},$$

$$\sigma^{\mathrm{SI}}_{VN} = \frac{\lambda^2_{HVV}}{16\pi m^4_H}\frac{m^4_N f^2_N}{(m_V + m_N)^2},$$

$$\sigma^{\mathrm{SI}}_{fN} = \frac{\lambda^2_{Hff}}{4\pi\Lambda^2 m^4_H}\frac{m^4_N m^2_f f^2_N}{(m_f + m_N)^2},$$

[JHEP 01 (2016) 172]

VBF H→inv + photon

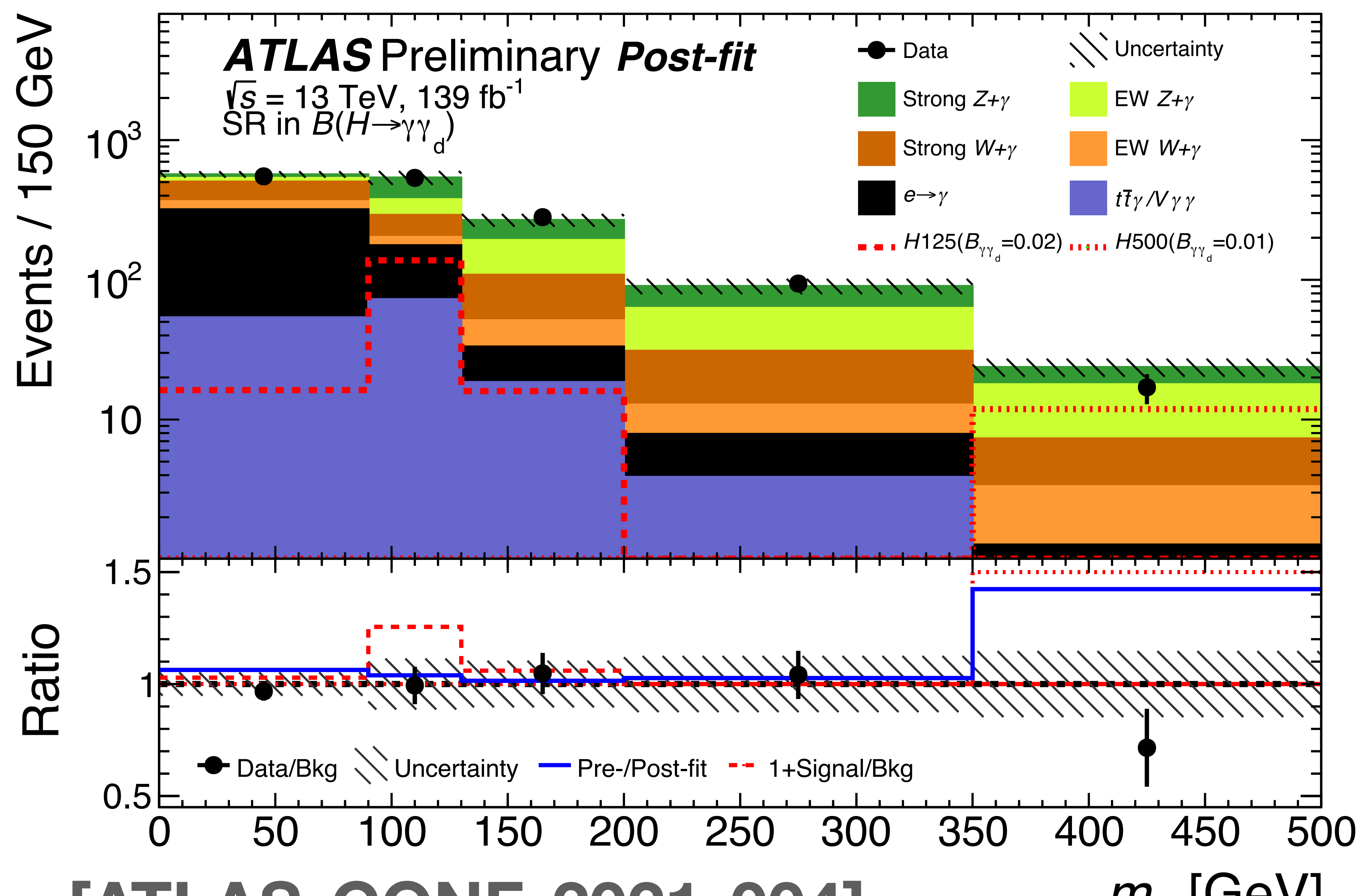

[ATLAS-CONF-2021-004]

Source	1σ Uncertainty on $\mathcal{B}_{\rm inv}$	1σ Uncertainty on $\mathcal{B}(H\rightarrow\gamma\gamma_d)$
Data stats.	0.106	0.0051
$V\gamma$+jets theory	0.056	0.0028
MC stats.	0.045	0.0026
Jet Scale and Resolution	0.045	0.0011
Photon	0.032	0.0011
$e\rightarrow\gamma$, jet→ e,γ Bkg.	0.026	0.0024
Pileup	0.025	0.0004
$W\gamma$+jets/$Z\gamma$+jets Norm.	0.021	0.0005
	0.012	0.0003
Signal theory	0.004	0.0010
Lepton	0.002	0.0008
Total	0.148	0.0071

Yields for the $\mathscr{B}$(inv) search

Process	Fake−e CR	$W^{\gamma}_{e\nu}$ CR	$W^{\gamma}_{\mu\nu}$ CR	$Z^{\gamma}_{\rm Rev.Cen.}$ CR	SR - DNN output score 0-0.25	0.25-0.6	0.6-0.8	0.8-1.0
Strong $Z\gamma$+jets	6± 7	0.5± 1.3	2± 2	53± 7	30±7	55± 12	10± 3	0.9± 0.3
EW $Z\gamma$+jets	0.6± 0.2	0.3± 0.2	0.5± 0.3	7± 1	14±2	39± 4	28± 4	10± 2
Strong $W\gamma$+jets	44± 8	46± 8	129± 18	21± 5	29± 10	30± 13	7± 3	0.1± 0.4
EW $W\gamma$+jets	20± 5	34± 6	64± 10	1.6± 0.4	5±1	8± 2	5± 1	1.1± 0.5
jet→ γ	1± 1	2± 2	3± 2	2± 2	2± 2	2± 2	0.8± 0.8	–
jet→ e	33± 16	5± 3	–	–	–	–	–	–
$e\rightarrow\gamma$	–	2.6± 0.4	2.9± 0.4	13± 1	9± 1	9± 1	1.9± 0.3	0.3± 0.1
$\gamma+$jet	–	–	–	0.7± 0.5	0.8± 0.6	0.6± 0.5	0.04± 0.03	–
$t\bar{t}\gamma/V\gamma\gamma$	3± 1	8± 2	12± 2	3± 1	4± 1	2± 1	0.9± 0.4	0.01± 0.01
Total Bkg	108± 10	97± 7	214± 14	101± 7	93± 8	146± 11	56± 6	13± 3
H ($\mathcal{B}_{\rm inv}=1$)	–	–	–	9± 1	7± 1	40± 5	39± 5	19± 2
Data	108	95	216	108	94	146	51	16
Data/Bkg	1.00± 0.14	0.98± 0.12	1.01± 0.09	0.99± 0.12	1.01± 0.14	1.00± 0.11	0.91± 0.16	1.19± 0.38

selection cuts

Variable	SR	$W^{\gamma}_{\mu\nu}$ CR	$W^{\gamma}_{e\nu}$ CR	$Z^{\gamma}_{\rm Rev.Cen.}$ CR	Fake−e CR
(j_1) [GeV]	>60				
(j_2) [GeV]	>50				
	2,3				
$N_{\rm b\text{-}jet}$	<2				
$\Delta\phi_{\rm jj}$	<2.5 [2.0]				
$\lvert\Delta\eta_{\rm jj}\rvert$	>3.0				
$\eta(j_1)\times\eta(j_2)$	<0				
C_3	<0.7				
$m_{\rm jj}$ []	>0.25				
[GeV]	>150	–	>80	>150	<80
$E_{\rm T}^{\rm miss,lep\text{-}rm}$ [GeV]	–	>150	>150	–	>150
$E_{\rm T}^{\rm jets,no\text{-}jvt}$ [GeV]	>130				
$\Delta\phi(j_i, E_{\rm T}^{\rm miss,lep\text{-}rm})$	>1.0				
N_{γ}	1				
(γ) [GeV]	>15, <110 [>15, $<\max(110, 0.733\times m_{\rm T})$]				
C_{γ}	>0.4	>0.4	>0.4	<0.4	>0.4
$\Delta\phi(\gamma, E_{\rm T}^{\rm miss,lep\text{-}rm})$	>1.8 [–]				
N_{ℓ}	0	1 μ	1 e	0	1 e
(ℓ) [GeV]	>30				

Presentation title